

1 **Bayesian updating on time intervals at different**
2 **magnitude thresholds in a marked point process and its**
3 **application to synthetic seismic activity**

4 **Hiroki Tanaka ¹and Ken Umeno ¹**

5 ¹Kyoto University, Yoshida-honmachi, Sakyo-ku, Kyoto-shi, JAPAN

6 **Key Points:**

- 7 • Bayesian updating for time intervals at different magnitude thresholds in marked
8 point process is discussed for large event forecasting
9 • Inverse probability density and its approximation functions are derived analyti-
10 cally for a time series with no correlation between events
11 • Forecasting of large events by Bayesian method is examined for the ETAS model
12 time series and its effectiveness is discussed statistically

Corresponding author: Hiroki Tanaka, tanaka.hiroki.43s@st.kyoto-u.ac.jp

Abstract

We present a Bayesian updating method on the inter-event times at different magnitude thresholds in a marked point process, toward the probabilistic forecasting of an upcoming large event using temporal information on smaller events. Bayes' theorem in a marked point process that yields the one-to-one relationship between intervals at lower and upper magnitude thresholds is presented. This theorem is extended to Bayesian updating for an uncorrelated marked point process that yields the relationship between multiple consecutive lower intervals and one upper interval. The inverse probability density function and its approximation function are derived. For the former, the condition for having a peak is shown. The latter is easier to apply to the time series of the ETAS model, and it consists of the kernel part, which includes the product of the conditional probabilities, and the correction term. The maximum point of the kernel part is shown to be not significantly affected by the correction term when applying the Bayesian updating to the ETAS model time series numerically. The occurrence time of the upcoming large event is estimated using this maximum point, and its accuracy is evaluated considering the relative error with the actual occurrence time. Moreover, forecasting is evaluated to be effective by the continuity of the updates with the accuracy within an acceptable range prior to the upcoming large event. Under these conditions, the statistical analysis indicates that forecasting is relatively effective immediately or long after the last major event in which stationarity is dominant in the time series.

Plain Language Summary

In order to forecast future large earthquakes, it is important to use as much information as possible on the seismic activity at hand. The number of small earthquakes is much larger than that of large earthquakes, and we propose a method to use this information to forecast probabilistically the timing of future large earthquakes. Theoretical analysis is performed on a simple time series. The theoretical results are applied to a seismic activity model, and it is shown that this method is relatively effective in forecasting the timing of future large events when stationary activity is dominant; in this model, either immediately after a large event or after sufficient time has passed since the last large event. Therefore, this method can be applied to reduce secondary disasters after a major earthquake and to evaluate the risk of earthquake occurrence over a long period of time.

1 Introduction

The probabilistic forecasting of the timing of future major earthquakes is important for seismic risk assessment. Therefore, it is necessary to effectively use the information on the temporal properties of seismic activity represented by a marked point process with the magnitude as the mark as indicated in Figure 1. A basic approach involves using the hazard rate based on the inter-event time distribution of earthquakes (Scholz, 2002). The inter-event time distribution is defined as a probability density function of the length of the interval between adjacent points in the point process determined by setting a magnitude threshold for the marked point process. For the magnitude threshold M (m), we denote the inter-event times using a variable τ_M (τ_m), and the inter-event time distribution it follows by $p_M(\tau_M)$ ($p_m(\tau_m)$).

The inter-event time distribution of earthquakes has been studied for not only risk assessment but also to understand the statistical nature of seismicity. For example, it has been studied with the aim to unify it with other established laws (Bak et al., 2002; Aizawa et al., 2013; Aizawa & Tsugawa, 2014) such as the GR law (Gutenberg & Richter, 1944) and the Omori–Utsu law (Omori, 1894; Utsu, 1961); further, its scaling universality (Corral, 2004) has been discussed using the ETAS model (Saichev & Sornette, 2006; Touati et al., 2009; Bottiglieri et al., 2010; Lippiello et al., 2012).

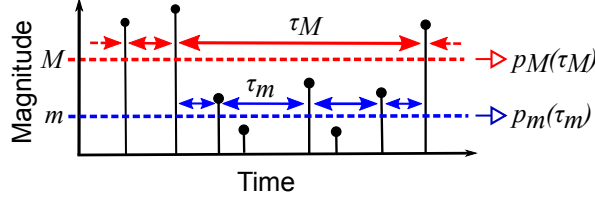


Figure 1. Schematic of a marked point process with the magnitude as a mark.

63 The ETAS model is a stochastic model that combines the GR and Omori–Utsu laws
 64 (Ogata, 1988, 1998); this model can generate a time series like that of the seismic ac-
 65 tivity. The ETAS model generates an inhomogeneous Poisson process with a history-dependent
 66 occurrence rate. Let t_j and M_j ($j \in \mathbb{N}$) represent the occurrence time and magnitude
 67 of the j -th event before time t ; then, the occurrence rate ($\lambda(t)$) at time t is given by

$$\lambda(t) = \lambda_0 + \sum_{j:t_j < t} \frac{K10^{\alpha(M_j - M_0)}}{(t - t_j + c)^{\theta+1}}. \quad (1)$$

68 The magnitude is generated randomly and independently obeying the GR law, $P(M) \propto$
 69 10^{-bM} . Here, M_0 represents the minimum magnitude and $(\lambda_0, K, \alpha, c, \theta, b)$ represent the
 70 parameters that characterize the activity. In particular, λ_0 represents the constant rate
 71 for background seismicity. The combination of the remaining parameters yields the branch-
 72 ing ratio $n_{\text{br}} = \frac{K}{\theta c^\theta} \frac{b}{b - \alpha}$ (when $\theta > 0$) (Helmstetter & Sornette, 2002) that determines
 73 the stationarity of the time series as well as the average number of aftershocks gener-
 74 ated by a mainshock (Helmstetter & Sornette, 2003).

75 The ETAS model provides a standard seismicity for detecting anomalous activity
 76 (Ogata, 1988). This model has been extended to a spatio-temporal version (Ogata, 1998),
 77 and its application to the evaluation of seismic risk has been studied actively. The con-
 78 ditional intensity function provides the risk of an event at a given time, space, and mag-
 79 nitude based on the history of seismic activity, which includes small earthquakes.

80 In the aforementioned probabilistic evaluation using the inter-event time distribu-
 81 tion, temporal information on events smaller than the magnitude threshold set on the
 82 marked point process is not utilized. Therefore, in this paper, we propose another ap-
 83 proach to probabilistically forecast major earthquakes based on the inter-event time dis-
 84 tribution while considering the temporal information on smaller events. This is achieved
 85 by utilizing a conditional probability that yields the statistical relationship between the
 86 inter-event times at different two magnitude thresholds (Tanaka & Aizawa, 2017).

For two magnitude thresholds m and $M (= m + \Delta m, \Delta m > 0)$ set in the time
 series, the conditional probability ($p_{mM}(\tau_m | \tau_M)$, hereafter referred to as the conditional
 probability density function) is defined as the probability density function of the length
 of a lower interval (τ_m) under the condition that it is included in the upper interval of
 length τ_M (Figure 1). Inter-event time distributions at magnitude thresholds m and M
 are connected by an integral equation with this conditional probability density function
 in its kernel (Tanaka & Aizawa, 2017). This integral equation is given as

$$N_m p_m(\tau_m) = N_M \int_{\tau_m}^{\infty} \frac{\tau_M}{\langle \langle \tau_m \rangle \rangle_{\tau_M}} p_{mM}(\tau_m | \tau_M) p_M(\tau_M) d\tau_M, \quad (2)$$

87 where N_m and N_M represent the total number of intervals at magnitude thresholds m
 88 and M , respectively. Further, $\langle \langle \tau_m \rangle \rangle_{\tau_M}$ represents the average of the conditional prob-
 89 ability density function, $\langle \langle \tau_m \rangle \rangle_{\tau_M} := \int_0^{\infty} \tau_m p_{mM}(\tau_m | \tau_M) d\tau_m$.

Thus, the conditional probability density function yields the statistical relation between inter-event times at different magnitude thresholds. This suggests that the information on the lower intervals can be utilized for estimating the length of the upper interval through the conditional probability density function. Given this context, we consider the Bayes' theorem and the Bayesian updating on the intervals at different magnitude thresholds in this paper; further, we report the results of the numerical analysis of the properties of the inverse probability density function (Tanaka & Umeno, 2021).

In §2, we derive the Bayes' theorem for intervals at different magnitude thresholds in the marked point process. In §3, the inverse probability density function is derived for the uncorrelated time series that corresponds to the background seismicity of the ETAS model. In §4, the Bayesian updating method is considered for the uncorrelated time series, and the inverse probability density function and its approximation function are derived. These functions are calculated numerically and compared in §5. In §6, Bayesian updating is applied to the time series of the ETAS model. The approximation function is examined numerically, and the property of the maximum point of its kernel part is analyzed statistically considering the effectiveness for forecasting. Finally, §7 presents additional discussions and conclusions.

2 Bayes' theorem for inter-event times at different magnitude thresholds

We consider the Bayes' theorem between the inter-event times at different magnitude thresholds (m and M) in a marked point process, and we derive the general relationship between the conditional probability density function $p_{mM}(\tau_m|\tau_M)$ and the inverse probability density function $p_{Mm}(\tau_M|\tau_m)$ (Tanaka & Umeno, 2021). Here $p_{Mm}(\tau_M|\tau_m)$ represents the probability density function of the upper interval under the condition that it includes a lower interval of length τ_m .

Let the total number of the pairs of the upper interval of length within $[\tau_M, \tau_M + d\tau_M)$ and the lower interval of length within $[\tau_m, \tau_m + d\tau_m)$ by $N_{mM}(\tau_M, \tau_m)$ (Figure 2). Hereafter, we express this $N_{mM}(\tau_M, \tau_m)$ as the number of the pairs of the intervals such that the length of the upper interval is τ_M and the length of the lower interval is τ_m , for simplicity, and other numbers of the intervals are expressed in the same way. $N_{mM}(\tau_M, \tau_m)$ can be represented in two ways:

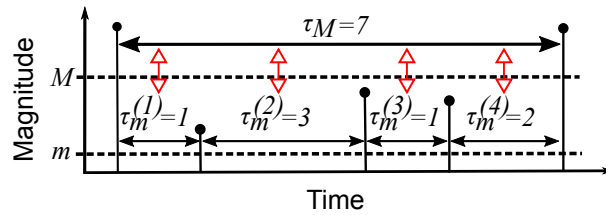


Figure 2. Schematic of the approach to count the number of pairs of upper and lower intervals whose lengths are τ_M and τ_m , respectively. Four pairs are shown in the figure, and $N_{mM}(7, 1) = 2$, $N_{mM}(7, 2) = 1$, and $N_{mM}(7, 3) = 1$.

1) Derive $N_{mM}(\tau_M, \tau_m)$ by counting the cumulative total number of the upper intervals of length τ_M that include the lower interval of length τ_m (Figure 3(a)). Among the N_m lower intervals in the time series, there are $N_m p_m(\tau_m) d\tau_m$ intervals of length τ_m . There exists only one upper interval that includes each of such lower intervals. The probability that the length of that upper interval is τ_M is given by $p_{Mm}(\tau_M|\tau_m) d\tau_M$. There-

fore

$$N_{mM}(\tau_M, \tau_m) = N_m p_m(\tau_m) p_{Mm}(\tau_M | \tau_m) d\tau_m d\tau_M. \quad (3)$$

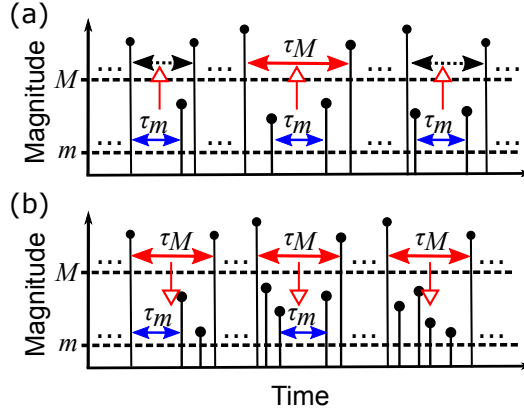


Figure 3. Schematic of the two approaches for calculating $N_{mM}(\tau_M, \tau_m)$. (a) The first approach involves counting the cumulative total number of the upper intervals of length τ_M that include the lower interval of length τ_m . (b) The second approach involves counting the number of the lower intervals of length τ_m included in the upper interval of length τ_M .

2) Derive $N_{mM}(\tau_M, \tau_m)$ by counting the total number of the lower intervals of length τ_m included in the upper interval of length τ_M (Figure 3(b)). The number of the upper intervals of length τ_M in the time series is $N_M p_M(\tau_M) d\tau_M$. Therefore, the number of the lower intervals included in these upper intervals is

$$N_M p_M(\tau_M) \frac{\tau_M}{\langle\langle\tau_m\rangle\rangle_{\tau_M}} d\tau_M.$$

Among them, the proportion of the lower intervals whose length is τ_m is $p_{mM}(\tau_m | \tau_M) d\tau_m$. Therefore

$$N_{mM}(\tau_M, \tau_m) = N_M p_M(\tau_M) \frac{\tau_M}{\langle\langle\tau_m\rangle\rangle_{\tau_M}} p_{mM}(\tau_m | \tau_M) d\tau_m d\tau_M. \quad (4)$$

From Equations (3) and (4)

$$N_m p_m(\tau_m) p_{Mm}(\tau_M | \tau_m) = N_M p_M(\tau_M) \frac{\tau_M}{\langle\langle\tau_m\rangle\rangle_{\tau_M}} p_{mM}(\tau_m | \tau_M). \quad (5)$$

By using the average intervals at each magnitude threshold

$$\begin{aligned} \langle\tau_m\rangle &:= \int_0^\infty \tau_m p_m(\tau_m) d\tau_m, \\ \langle\tau_M\rangle &:= \int_0^\infty \tau_M p_M(\tau_M) d\tau_M, \end{aligned}$$

and $N_M/N_m = \langle\tau_m\rangle/\langle\tau_M\rangle$, Equation (5) is rewritten as

$$p_{Mm}(\tau_M | \tau_m) = \left(\frac{\langle\tau_m\rangle}{\langle\tau_M\rangle} \frac{\tau_M}{\langle\langle\tau_m\rangle\rangle_{\tau_M}} \right) \frac{p_{mM}(\tau_m | \tau_M) p_M(\tau_M)}{p_m(\tau_m)}. \quad (6)$$

Equation (6) can be considered as the Bayes' theorem for a marked point process. The parenthesized part is from the difference in the number of intervals for each magnitude threshold ($\langle\tau_m\rangle/\langle\tau_M\rangle$) and the inclusion relationship between the upper and lower

intervals $(\tau_M / \langle \tau_m \rangle_{\tau_M})$, i.e., a lower interval is always included in only one upper interval, whereas an upper interval includes $\tau_M / \langle \tau_m \rangle_{\tau_M}$ lower intervals on average. This part disappears by using generalized probability density functions

$$\begin{aligned} z_m(\tau_m) &:= \frac{\tau_m}{\langle \tau_m \rangle} p_m(\tau_m), \\ z_M(\tau_M) &:= \frac{\tau_M}{\langle \tau_M \rangle} p_M(\tau_M), \\ z_{mM}(\tau_m | \tau_M) &:= \frac{\tau_m}{\langle \tau_m \rangle_{\tau_M}} p_{mM}(\tau_m | \tau_M). \end{aligned}$$

These functions satisfy the normalization condition of the probability density function. Equations (2) and (6) are simplified as

$$z_m(\tau_m) = \int_0^\infty z_{mM}(\tau_m | \tau_M) z_M(\tau_M) d\tau_M, \quad (7)$$

$$p_{mM}(\tau_M | \tau_m) = \frac{z_{mM}(\tau_m | \tau_M) z_M(\tau_M)}{z_m(\tau_m)}. \quad (8)$$

121 These equations indicate that $p_{mM}(\tau_M | \tau_m)$ satisfies the normalization condition.

122 3 Bayes' theorem for uncorrelated time series

In this section, we derive $p_{mM}(\tau_M | \tau_m)$ for an uncorrelated time series generated by the ETAS model with $\lambda(t) \equiv \lambda_0$ (Tanaka & Umeno, 2021). In this case, the magnitudes and inter-event times obey the following probability density functions independently.

$$P(m) \propto 10^{-bm}, \quad (9)$$

$$p_m(\tau_m) = \frac{1}{\langle \tau_m \rangle} e^{-\frac{\tau_m}{\langle \tau_m \rangle}}. \quad (10)$$

First, we derive $p_{mM}(\tau_m | \tau_M)$, which can be expressed generally as

$$p_{mM}(\tau_m | \tau_M) = \frac{\sum_{i=1}^{\infty} i \rho_{mM}(\tau_m | i, \tau_M) \Psi_{mM}(i | \tau_M)}{\sum_{i=1}^{\infty} i \Psi_{mM}(i | \tau_M)}, \quad (11)$$

123 where $i \in \mathbb{Z}$ represents the number of lower intervals included in the upper interval of
 124 length τ_M ; $\Psi_{mM}(i | \tau_M)$ represents the probability mass function of such i under the con-
 125 dition that the length of the upper interval is τ_M ; and $\rho_{mM}(\tau_m | i, \tau_M)$ represents the prob-
 126 ability density function of the length of a lower interval given that the length of the up-
 127 per interval is τ_M and the number of the lower intervals in it is i . We can calculate the
 128 conditional probability density function and other related amounts when we know these
 129 functions.

In the case of the uncorrelated time series, these functions can be obtained as fol-
 lows. For the selected stationary Poisson process, the average number of events included
 in the upper interval of length τ_M is $(\tau_M / \langle \tau_m \rangle - \tau_M / \langle \tau_M \rangle)$, because no event greater
 than M occurs in the interval considered, and therefore, $\tau_M / \langle \tau_M \rangle$ -events larger than M
 occurring in the interval of length τ_M on average must be excluded from the average num-
 ber $\tau_M / \langle \tau_m \rangle$ of events occurring in the interval of length τ_M . Then, the average occur-
 rence rate in the upper interval of length τ_M is $(1 / \langle \tau_m \rangle - 1 / \langle \tau_M \rangle)$. The number of events
 with $m < \text{magnitude} \leq M$ in τ_M is one less than that of the lower intervals, and there-
 fore, the probability of including i lower intervals is equal to the probability of includ-
 ing $(i - 1)$ events with an average occurrence rate $(1 / \langle \tau_m \rangle - 1 / \langle \tau_M \rangle)$. Therefore

$$\Psi_{mM}(i | \tau_M) = \frac{\left(A_{\Delta m} \frac{\tau_M}{\langle \tau_M \rangle} \right)^{i-1}}{(i-1)!} e^{-A_{\Delta m} \frac{\tau_M}{\langle \tau_M \rangle}}, \quad (12)$$

where

$$\begin{aligned} A_{\Delta m} &:= \frac{\langle \tau_M \rangle}{\langle \tau_m \rangle} - 1 \\ &= 10^{b\Delta m} - 1. \end{aligned}$$

130 The second transformation in the above equation does not strictly hold for a time se-
131 ries with a finite number of events because the number of the events is different from that
132 of the intervals by 1. However, we consider that the statistical properties are for infinite
133 samples, and in a time series containing an infinite number of events, the two are equiv-
134 alent and the equality holds.

The other function $\rho_{mM}(\tau_m|i, \tau_M)$ is obtained as follows. For $i = 1$

$$\rho_{mM}(\tau_m|1, \tau_M) = \delta(\tau_M - \tau_m), \quad (13)$$

where $\delta(x)$ represents the Dirac's delta function. For $i \geq 2$ (Webb, 1974)

$$\rho_{mM}(\tau_m|i, \tau_M) = \frac{(i-1)}{\tau_M} \left(1 - \frac{\tau_m}{\tau_M}\right)^{i-2} \theta(\tau_M - \tau_m), \quad (14)$$

135 where $\theta(x)$ represents the unit step function that returns 1 for $x > 0$ and 0 for $x \leq$
136 0.

From Equations (12)–(14), $p_{mM}(\tau_m|\tau_M)$ is derived as (Appendix A)

$$p_{mM}(\tau_m|\tau_M) = \frac{e^{-A_{\Delta m} \frac{\tau_M}{\langle \tau_m \rangle}} \delta(\tau_M - \tau_m) + \frac{A_{\Delta m}}{\langle \tau_m \rangle} e^{-A_{\Delta m} \frac{\tau_m}{\langle \tau_m \rangle}} \left\{ A_{\Delta m} \frac{\tau_M - \tau_m}{\langle \tau_M \rangle} + 2 \right\} \theta(\tau_M - \tau_m)}{\left(A_{\Delta m} \frac{\tau_M}{\langle \tau_M \rangle} + 1 \right)}. \quad (15)$$

137 This conditional probability composed of Equations (12)–(14) certainly has exponential
138 distributions as the solution of Equation (2) (Appendix A).

Second, we derive $p_{Mm}(\tau_M|\tau_m)$. From Equations (10) and (15), $p_{Mm}(\tau_M|\tau_m)$ is obtained as (Appendix A)

$$p_{Mm}(\tau_M|\tau_m) = \frac{e^{-\frac{\tau_M - \tau_m}{\langle \tau_m \rangle}} \delta(\tau_M - \tau_m) + \frac{A_{\Delta m}}{\langle \tau_M \rangle} e^{-\frac{\tau_M - \tau_m}{\langle \tau_M \rangle}} \left\{ A_{\Delta m} \frac{\tau_M - \tau_m}{\langle \tau_M \rangle} + 2 \right\} \theta(\tau_M - \tau_m)}{(A_{\Delta m} + 1)^2}. \quad (16)$$

We emphasize that $p_{Mm}(\tau_M|\tau_m)$ has a peak at

$$\tau_M^{\max} = \tau_m + \langle \tau_M \rangle \left(1 - \frac{2}{A_{\Delta m}} \right), \quad (17)$$

when the next condition is satisfied (Appendix A).

$$\Delta m > \frac{\log_{10} 3}{b}. \quad (18)$$

139 4 Bayesian updating for uncorrelated time series

140 The Bayes' theorem shows a one-to-one relationship between an upper and a lower
141 interval. In this section, we extend it to the relationship between an upper interval and
142 multiple consecutive lower intervals by considering Bayesian updating for the uncorre-
143 lated time series (Tanaka & Umeno, 2021). We derive the inverse probability density func-
144 tion $p_{Mm}(\tau_M|\tau_m^{(1)}, \dots, \tau_m^{(n)})$, as well as its approximation function, for the upper inter-
145 val under the condition that it includes the consecutive lower intervals of lengths $\{\tau_m^{(1)}, \dots, \tau_m^{(n)}\}$.

146

4.1 Inverse probability density function

147

148

149

150

As in §2, we derive the inverse probability density function by expressing the total number of combinations of the upper interval of length τ_M and the consecutive lower intervals of lengths $\{\tau_m^{(1)}, \dots, \tau_m^{(n)}\}$ included in it denoted by $N_{mM}(\tau_M, \tau_m^{(1)}, \dots, \tau_m^{(n)})$ in two ways.

First, we derive $N_{mM}(\tau_M, \tau_m^{(1)}, \dots, \tau_m^{(n)})$ by counting the cumulative total number of the upper intervals of length τ_M that include the consecutive lower intervals of lengths $\{\tau_m^{(1)}, \dots, \tau_m^{(n)}\}$ (Figure 4(a)). We begin with the case $n = 2$. The intervals in the uncorrelated time series emerge independently, and therefore, the total number of the two consecutive lower intervals of lengths $\tau_m^{(1)}$ and $\tau_m^{(2)}$ is

$$N_m p_m(\tau_m^{(1)}) p_m(\tau_m^{(2)}) d\tau_m^2.$$

Among them, some pairs do not belong to the same upper interval (the case of (3) in Figure 4(a)). In that case, the magnitude of the event sandwiched between the two lower intervals is larger than M . In the uncorrelated time series, the proportion that the consecutive lower intervals belong to the same upper interval equals to the probability that the magnitude of the event sandwiched between the two lower intervals is smaller than M . It is given by the GR law as

$$\begin{aligned} 1 - \frac{P(M)}{P(m)} &= 1 - 10^{-b\Delta m} \\ &= 1 - \frac{\langle \tau_m \rangle}{\langle \tau_M \rangle}. \end{aligned}$$

Therefore

$$N_{mM}(\tau_M, \tau_m^{(1)}, \tau_m^{(2)}) = N_m \left(1 - \frac{\langle \tau_m \rangle}{\langle \tau_M \rangle}\right) p_m(\tau_m^{(1)}) p_m(\tau_m^{(2)}) p_{Mm}(\tau_M | \tau_m^{(1)}, \tau_m^{(2)}) d\tau_m^2 d\tau_M. \quad (19)$$

Equation (19) is generalized for $n(\geq 2)$ consecutive lower intervals.

$$\begin{aligned} &N_{mM}(\tau_M, \tau_m^{(1)}, \dots, \tau_m^{(n)}) \\ &= N_m \left(1 - \frac{\langle \tau_m \rangle}{\langle \tau_M \rangle}\right)^{n-1} \left(\prod_{i=1}^n p_m(\tau_m^{(i)})\right) p_{Mm}(\tau_M | \tau_m^{(1)}, \dots, \tau_m^{(n)}) d\tau_m^n d\tau_M. \quad (20) \end{aligned}$$

Second, we derive $N_{mM}(\tau_M, \tau_m^{(1)}, \dots, \tau_m^{(n)})$ by counting the total number of the consecutive lower intervals of lengths $\{\tau_m^{(1)}, \dots, \tau_m^{(n)}\}$ included in the upper interval of length τ_M (Figure 4(b)). To this end, we start with the case $n = 2$ again (Figure 4(b)). When the upper interval of length τ_M includes $i(\geq 2)$ lower intervals, the first interval of the two consecutive lower intervals is selected from $(i-1)$ intervals except for the rightmost one. The probability that this first interval has length $\tau_m^{(1)}$ is $\rho_{mM}(\tau_m^{(1)} | i, \tau_M) d\tau_m$. The second lower interval is fixed at adjacent to the first one. This second interval is one of the $(i-1)$ intervals that divide the remaining length $\tau_M - \tau_m^{(1)}$, and therefore, the probability that the second interval has length $\tau_m^{(2)}$ is $\rho_{mM}(\tau_m^{(2)} | i-1, \tau_M - \tau_m^{(1)}) d\tau_m$. Thus, considering all $i(\geq 2)$

$$\begin{aligned} &N_{mM}(\tau_M, \tau_m^{(1)}, \tau_m^{(2)}) \\ &= N_M p_M(\tau_M) d\tau_M \sum_{i=2}^{\infty} (i-1) \Psi_{mM}(i | \tau_M) \rho_{mM}(\tau_m^{(1)} | i, \tau_M) \rho_{mM}(\tau_m^{(2)} | i-1, \tau_M - \tau_m^{(1)}) d\tau_m^2. \quad (21) \end{aligned}$$

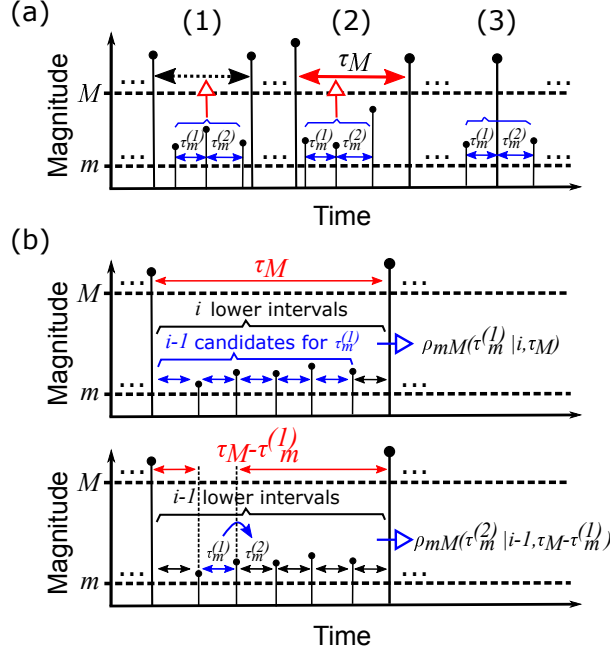


Figure 4. Schematic of the two approaches to calculate $N_{mM}(\tau_M, \tau_m^{(1)}, \tau_m^{(2)})$. (a) The first approach involves counting the cumulative total number of the upper intervals of length τ_M that include the consecutive lower intervals of lengths $\{\tau_m^{(1)}, \tau_m^{(2)}\}$. (b) The second approach involves counting the number of the consecutive lower intervals of lengths $\{\tau_m^{(1)}, \tau_m^{(2)}\}$ included in the upper interval of length τ_M .

Equation (21) is generalized for the case $n(\geq 2)$ lower intervals as

$$\begin{aligned}
 N_{mM}(\tau_M, \tau_m^{(1)}, \dots, \tau_m^{(n)}) &= N_M p_M(\tau_M) d\tau_M \\
 &\times \sum_{i=n}^{\infty} (i-n+1) \Psi_{mM}(i|\tau_M) \rho_{mM}(\tau_m^{(1)}|i, \tau_M) \prod_{j=2}^n \rho_{mM}\left(\tau_m^{(j)}|i-j+1, \tau_M - \sum_{k=1}^{j-1} \tau_m^{(k)}\right) d\tau_m^n.
 \end{aligned} \tag{22}$$

From Equations (20) and (22), $p_{Mm}(\tau_M|\tau_m^{(1)}, \dots, \tau_m^{(n)})$ is derived as

$$\begin{aligned}
 p_{Mm}(\tau_M|\tau_m^{(1)}, \dots, \tau_m^{(n)}) &= \frac{\langle \tau_m \rangle}{\langle \tau_M \rangle} \frac{1}{\left(1 - \frac{\langle \tau_m \rangle}{\langle \tau_M \rangle}\right)^{n-1}} \frac{p_M(\tau_M)}{\prod_{i=1}^n p_m(\tau_m^{(i)})} \\
 &\times \sum_{i=n}^{\infty} (i-n+1) \Psi_{mM}(i|\tau_M) \rho_{mM}(\tau_m^{(1)}|i, \tau_M) \prod_{j=2}^n \rho_{mM}\left(\tau_m^{(j)}|i-j+1, \tau_M - \sum_{k=1}^{j-1} \tau_m^{(k)}\right).
 \end{aligned} \tag{23}$$

Furthermore, the explicit form of the inverse probability density function is derived by substituting Equations (10) and (12)–(14) into Equation (23) as (Appendix B)

$$\begin{aligned}
 p_{Mm}(\tau_M|\tau_m^{(1)}, \dots, \tau_m^{(n)}) &= \left(\frac{\langle \tau_m \rangle}{\langle \tau_M \rangle}\right)^2 \left[e^{-\frac{\tau_M - \sum_{i=1}^n \tau_m^{(i)}}{\langle \tau_m \rangle}} \delta\left(\tau_M - \sum_{i=1}^n \tau_m^{(i)}\right) \right. \\
 &\left. + \frac{A_{\Delta m}}{\langle \tau_M \rangle} e^{-\frac{\tau_M - \sum_{i=1}^n \tau_m^{(i)}}{\langle \tau_M \rangle}} \left\{ \frac{A_{\Delta m}}{\langle \tau_M \rangle} \left(\tau_M - \sum_{i=1}^n \tau_m^{(i)}\right) + 2 \right\} \theta\left(\tau_M - \sum_{i=1}^n \tau_m^{(i)}\right) \right].
 \end{aligned} \tag{24}$$

151 Equation (24) includes the case $n = 1$ (Equation (16)). In addition, Equation (24)
 152 is identical to Equation (16) when τ_m is replaced with $\mathcal{T} := \sum_{i=1}^n \tau_m^{(i)}$; this implies that
 153 the occurrence pattern of small events does not affect that of upper intervals. This seems
 154 natural for the uncorrelated time series.

The same property as Equations (17) and (18) holds for $p_{Mm}(\tau_M | \tau_m^{(1)}, \dots, \tau_m^{(n)})$;
 it has a peak at

$$\tau_M^{\max} = \mathcal{T} + \langle \tau_M \rangle \frac{\frac{\langle \tau_M \rangle}{\langle \tau_m \rangle} - 3}{\frac{\langle \tau_M \rangle}{\langle \tau_m \rangle} - 1} (> \mathcal{T}),$$

under the condition

$$\Delta m > \frac{\log_{10} 3}{b}. \quad (25)$$

155 In the above mentioned Bayesian updating, the position of the consecutive lower
 156 intervals in an upper interval is not restricted. However, update can be started only from
 157 the lower interval immediately after the event with the magnitude above M . In such a
 158 method, the inverse probability density function is different from Equation (24) (Appendix
 159 C). At a glance, this updating method seems suitable under the situation wherein the
 160 information on the lower intervals observed one after another is imported sequentially;
 161 however, seismic catalogs are known to be incomplete immediately after a large earth-
 162 quake. In that case, the lower intervals should be considered not from the leftmost one
 163 but from somewhere else. Therefore, in the present paper, we limit ourselves to exam-
 164 ine the property of the inverse probability density function of the unrestricted updat-
 165 ing method that is more appropriate for application to earthquake catalogs.

166 4.2 Approximation function of inverse probability density function

167 Equation (23) indicates that new information on the lower intervals cannot be added
 168 by the product of the conditional probabilities as is usual in Bayesian updating. In this
 169 sub-section, we derive its approximation function with a convenient form applicable to
 170 the time series with correlations between events.

To this end, we use the approximate derivation of $N_{mM}(\tau_M, \tau_m^{(1)}, \dots, \tau_m^{(n)})$ described
 below instead of the second approach for deriving Equation (22). In the following, the
 upper and the lower consecutive intervals are assumed to satisfy

$$\tau_M \geq \sum_{i=1}^n \tau_m^{(i)}. \quad (26)$$

First, consider the case $n = 2$. There are $N_{MPM}(\tau_M) d\tau_M$ upper intervals of length
 τ_M in the time series. These upper intervals are as shown in Figure 5(a), and we use them
 to generate a new time series by connecting them in the order of appearance as in Fig-
 ure 5(b). Let the number of the consecutive lower intervals of lengths $\{\tau_m^{(1)}, \tau_m^{(2)}\}$ in this
 new time series be denoted by $N'_{mM}(\tau_m^{(1)}, \tau_m^{(2)} | \tau_M)$. The total number of the lower in-
 tervals in this new time series is given as

$$N_{MPM}(\tau_M) \frac{\tau_M}{\langle \langle \tau_m \rangle \rangle_{\tau_M}} d\tau_M.$$

Therefore, based on the assumption that $\tau_m^{(1)}$ and $\tau_m^{(2)}$ emerge independently, $N'_{mM}(\tau_m^{(1)}, \tau_m^{(2)} | \tau_M)$
 is approximately calculated as

$$N'_{mM}(\tau_m^{(1)}, \tau_m^{(2)} | \tau_M) \approx N_{MPM}(\tau_M) \frac{\tau_M}{\langle \langle \tau_m \rangle \rangle_{\tau_M}} p_{mM}(\tau_m^{(1)} | \tau_M) p_{mM}(\tau_m^{(2)} | \tau_M) d\tau_m^2 d\tau_M. \quad (27)$$

171 $N'_{mM}(\tau_m^{(1)}, \tau_m^{(2)} | \tau_M)$ is not equivalent to $N_{mM}(\tau_M, \tau_m^{(1)}, \tau_m^{(2)})$ because $N'_{mM}(\tau_m^{(1)}, \tau_m^{(2)} | \tau_M)$
 172 includes cases where the two consecutive lower intervals do not belong to the same up-

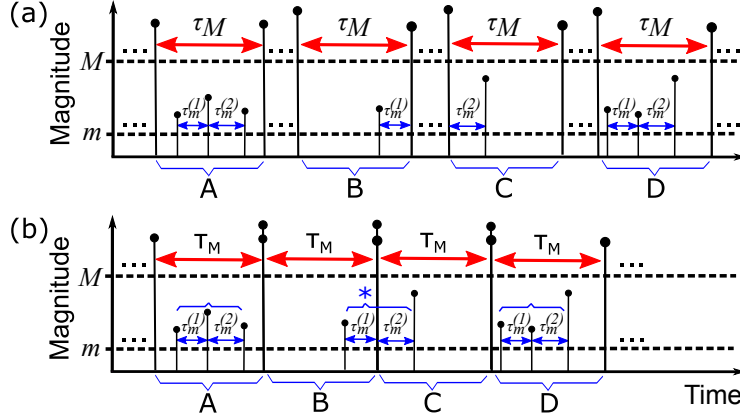


Figure 5. Schematic of another approach to count the total number of consecutive lower intervals of lengths $\tau_m^{(1)}$ and $\tau_m^{(2)}$ included in the upper interval of length τ_M . (a) First, pick up all upper intervals of length τ_M from the time series. (b) Second, generate new time series by connecting these upper intervals in the order of appearance. Third, $N'_{mM}(\tau_m^{(1)}, \tau_m^{(2)} | \tau_M)$ is calculated by counting the total number of the consecutive lower intervals of lengths $\{\tau_m^{(1)}, \tau_m^{(2)}\}$ in this new time series. In this counting process, an approximate calculation using the product of the conditional probability is conducted. Finally, $N_{mM}(\tau_M, \tau_m^{(1)}, \tau_m^{(2)})$ is obtained by excluding such pairs where the two consecutive lower intervals are not included in the same upper interval (the cases indicated with *) from $N'_{mM}(\tau_m^{(1)}, \tau_m^{(2)} | \tau_M)$.

173 per interval (the case indicated by * in Figure 5(b)). Therefore, it is necessary to count
 174 such cases in the time series, and subtract them from $N'_{mM}(\tau_m^{(1)}, \tau_m^{(2)} | \tau_M)$.

These cases to exclude occur when an upper interval of length τ_M whose rightmost lower interval has length $\tau_m^{(1)}$ is adjacent to the left of another upper interval whose leftmost lower interval has length $\tau_m^{(2)}$. The probability density that the length of the rightmost or leftmost lower interval of the upper interval of length τ_M is τ_m is, because the position of the rightmost or leftmost interval is confirmed among the i -lower intervals, calculated as

$$\begin{aligned} P^R(\tau_m | \tau_M) &= P^L(\tau_m | \tau_M) \\ &= \sum_{i=1}^{\infty} \Psi_{mM}(i | \tau_M) \rho_{mM}(\tau_m | i, \tau_M). \end{aligned} \quad (28)$$

Here, the probability density for the rightmost lower interval is denoted by $P^R(\tau_m | \tau_M)$, and the leftmost by $P^L(\tau_m | \tau_M)$. Equation (28) can be explicitly written using Equations (12)–(14) as (Appendix D)

$$\begin{aligned} P^R(\tau_m | \tau_M) &= P^L(\tau_m | \tau_M) \\ &= e^{-A_{\Delta m} \frac{\tau_M}{\langle \tau_M \rangle}} \delta(\tau_M - \tau_m) + \frac{A_{\Delta m}}{\langle \tau_M \rangle} e^{-A_{\Delta m} \frac{\tau_m}{\langle \tau_M \rangle}} \theta(\tau_M - \tau_m). \end{aligned} \quad (29)$$

By using $P^L(\tau_m | \tau_M)$ and $P^R(\tau_m | \tau_M)$, the number of cases to exclude can be expressed for a sufficiently large N_M (because $N_M p_M(\tau_M) d\tau_M$ in Equation (30) is precisely $N_M p_M(\tau_M) d\tau_M - 1$) as

$$N_M p_M(\tau_M) P^R(\tau_m^{(1)} | \tau_M) P^L(\tau_m^{(2)} | \tau_M) d\tau_m^2 d\tau_M. \quad (30)$$

Therefore, $N_{mM}(\tau_M, \tau_m^{(1)}, \tau_m^{(2)})$ is approximately derived as

$$N_{mM}(\tau_M, \tau_m^{(1)}, \tau_m^{(2)}) \approx N_M p_M(\tau_M) \times \left(\frac{\tau_M}{\langle\langle\tau_m\rangle\rangle_{\tau_M}} p_{mM}(\tau_m^{(1)}|\tau_M) p_{mM}(\tau_m^{(2)}|\tau_M) - P^R(\tau_m^{(1)}|\tau_M) P^L(\tau_m^{(2)}|\tau_M) \right) d\tau_m^2 d\tau_M. \quad (31)$$

Next, we consider the case $n(\geq 3)$. Equation (27) is generalized as

$$N'_{mM}(\tau_m^{(1)}, \dots, \tau_m^{(n)}|\tau_M) \approx N_M p_M(\tau_M) \frac{\tau_M}{\langle\langle\tau_m\rangle\rangle_{\tau_M}} \left(\prod_{i=1}^n p_{mM}(\tau_m^{(i)}|\tau_M) \right) d\tau_m^n d\tau_M. \quad (32)$$

From this $N'_{mM}(\tau_m^{(1)}, \dots, \tau_m^{(n)}|\tau_M)$, the cases wherein the consecutive lower intervals of lengths $\{\tau_m^{(1)}, \dots, \tau_m^{(n)}\}$ are not included in the same upper interval need to be excluded. Considering the condition of Equation (26), a sequence of consecutive lower intervals is divided by only one boundary event with a magnitude above M (Figure 6). Let the probability that the rightmost or leftmost lower intervals of the upper interval of length τ_M is $\{\tau_m^{(1)}, \dots, \tau_m^{(l)}\}$ ($l \geq 2$) be $P(\tau_m^{(1)}, \dots, \tau_m^{(l)}|\tau_M)$. Then, as the position of the rightmost or leftmost lower intervals is confirmed among the $i(\geq l)$ lower intervals, $P(\tau_m^{(1)}, \dots, \tau_m^{(l)}|\tau_M)$ is

$$P(\tau_m^{(1)}, \dots, \tau_m^{(l)}|\tau_M) = \sum_{i=l}^{\infty} \Psi_{mM}(i|\tau_M) \rho_{mM}(\tau_m^{(1)}|i, \tau_M) \prod_{j=2}^l \rho_{mM} \left(\tau_m^{(j)}|i - j + 1, \tau_M - \sum_{k=1}^{j-1} \tau_m^{(k)} \right). \quad (33)$$

By substituting Equations (12)–(14) into Equation (33) (Appendix E)

$$P(\tau_m^{(1)}, \dots, \tau_m^{(l)}|\tau_M) = \prod_{i=1}^l P_i(\tau_m^{(i)}|\tau_M), \text{ where } P_i(\tau_m^{(i)}|\tau_M) := \left(\frac{A\Delta m}{\langle\tau_M\rangle} \right) e^{-A\Delta m \frac{\tau_m^{(i)}}{\langle\tau_M\rangle}}. \quad (34)$$

There are $(n - 1)$ possible choices for the boundary position of the consecutive lower intervals (Figure 6(a)), each with an equal probability $\prod_{i=1}^n P_i$. The number of consecutive upper intervals in the new time series is almost $N_M p_M(\tau_M) d\tau_M$, and therefore, the number of cases to be excluded is

$$N_M p_M(\tau_M) (n - 1) \left(\prod_{i=1}^n P_i(\tau_m^{(i)}|\tau_M) \right) d\tau_m^n d\tau_M.$$

Then

$$N_{mM}(\tau_M, \tau_m^{(1)}, \dots, \tau_m^{(n)}) \approx N_M p_M(\tau_M) \left\{ \frac{\tau_M}{\langle\langle\tau_m\rangle\rangle_{\tau_M}} \prod_{i=1}^n p_{mM}(\tau_m^{(i)}|\tau_M) - (n - 1) \prod_{i=1}^n P_i(\tau_m^{(i)}|\tau_M) \right\} d\tau_m^n d\tau_M. \quad (35)$$

Therefore, from Equations (20) and (35), the approximation function ($p_{Mm}^{\text{approx}}(\tau_M|\tau_m^{(1)}, \dots, \tau_m^{(n)})$) of the inverse probability density function is derived as

$$p_{Mm}^{\text{approx}}(\tau_M|\tau_m^{(1)}, \dots, \tau_m^{(n)}) = \frac{\langle\tau_m\rangle}{\langle\tau_M\rangle} \frac{1}{\left(1 - \frac{\langle\tau_m\rangle}{\langle\tau_M\rangle}\right)^{n-1}} \frac{\tau_M}{\langle\langle\tau_m\rangle\rangle_{\tau_M}} \left(\prod_{i=1}^n \frac{p_{mM}(\tau_m^{(i)}|\tau_M)}{p_m(\tau_m^{(i)})} \right) p_M(\tau_M) - \frac{\langle\tau_m\rangle}{\langle\tau_M\rangle} \frac{(n - 1)}{\left(1 - \frac{\langle\tau_m\rangle}{\langle\tau_M\rangle}\right)^{n-1}} \left(\prod_{i=1}^n \frac{P_i(\tau_m^{(i)}|\tau_M)}{p_m(\tau_m^{(i)})} \right) p_M(\tau_M). \quad (36)$$

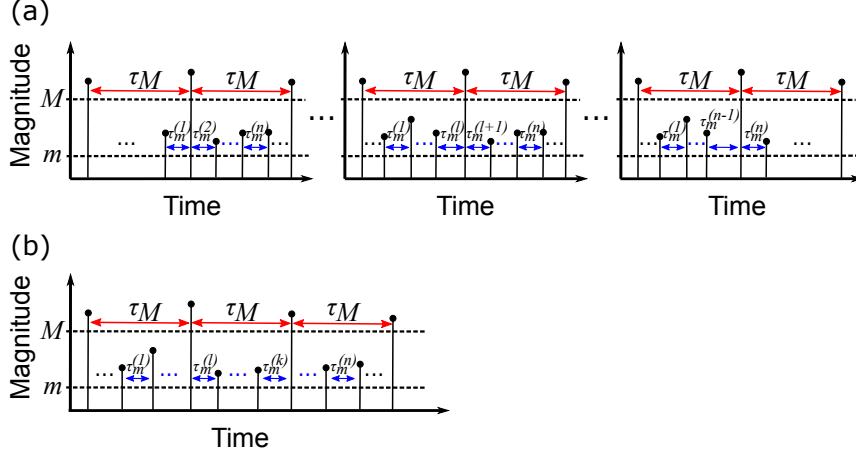


Figure 6. Schematic of the patterns of the consecutive lower intervals of lengths $\{\tau_m^{(1)}, \dots, \tau_m^{(n)}\}$ excluded from $N'_{mM}(\tau_m^{(1)}, \dots, \tau_m^{(n)} | \tau_M)$. (a) There are $(n - 1)$ ways to divide the sequence of lower intervals by the event with a magnitude greater than M at the boundary of the upper intervals of length τ_M . (b) The sequence can not be divided by more than one boundary according to condition (26).

Equation (36) is composed of two parts: the first term of the r.h.s. involves the product of the conditional probability density functions, and we refer to this part as the kernel part of the approximation function ($p_{Mm}^{\text{kernel}}(\tau_M | \tau_m^{(1)}, \dots, \tau_m^{(n)})$) hereafter.

$$p_{Mm}^{\text{kernel}}(\tau_M | \tau_m^{(1)}, \dots, \tau_m^{(n)}) = \frac{\langle \tau_m \rangle}{\langle \tau_M \rangle} \frac{1}{\left(1 - \frac{\langle \tau_m \rangle}{\langle \tau_M \rangle}\right)^{n-1}} \frac{\tau_M}{\langle \tau_M \rangle} \left(\prod_{i=1}^n \frac{p_{mM}(\tau_m^{(i)} | \tau_M)}{p_m(\tau_m^{(i)})} \right) p_M(\tau_M). \quad (37)$$

The second term of the r.h.s. is referred to as the correction term, and we denote the part other than $(n - 1)$ by $p_{Mm}^{\text{correct}}(\tau_M | \tau_m^{(1)}, \dots, \tau_m^{(n)})$ as

$$\text{correction term} = (n - 1) p_{Mm}^{\text{correct}}(\tau_M | \tau_m^{(1)}, \dots, \tau_m^{(n)}), \quad (38)$$

$$\text{where } p_{Mm}^{\text{correct}}(\tau_M | \tau_m^{(1)}, \dots, \tau_m^{(n)}) = \frac{\langle \tau_m \rangle}{\langle \tau_M \rangle} \frac{1}{\left(1 - \frac{\langle \tau_m \rangle}{\langle \tau_M \rangle}\right)^{n-1}} \left(\prod_{i=1}^n \frac{P_i(\tau_m^{(i)} | \tau_M)}{p_m(\tau_m^{(i)})} \right) p_M(\tau_M).$$

Equation (36) can be explicitly written as (Appendix F)

$$p_{Mm}^{\text{approx}}(\tau_M | \tau_m^{(1)}, \dots, \tau_m^{(n)}) = \frac{\langle \tau_m \rangle}{\langle \tau_M \rangle^2} \left(1 - \frac{\langle \tau_m \rangle}{\langle \tau_M \rangle}\right) \left(A_{\Delta m} \frac{\tau_M}{\langle \tau_M \rangle} + 1\right) e^{-\frac{\tau_M - \sum_{i=1}^n \tau_m^{(i)}}{\langle \tau_M \rangle}} \\ \times \prod_{i=1}^n \left\{ 1 - \left(\frac{\tau_m^{(i)} - \frac{\langle \tau_M \rangle}{A_{\Delta m}}}{\tau_M + \frac{\langle \tau_M \rangle}{A_{\Delta m}}} \right) \right\} - \frac{\langle \tau_m \rangle}{\langle \tau_M \rangle^2} \left(1 - \frac{\langle \tau_m \rangle}{\langle \tau_M \rangle}\right) (n - 1) e^{-\frac{\tau_M - \sum_{i=1}^n \tau_m^{(i)}}{\langle \tau_M \rangle}}. \quad (39)$$

The kernel part is explicitly expressed as

$$p_{Mm}^{\text{kernel}}(\tau_M | \tau_m^{(1)}, \dots, \tau_m^{(n)}) = \frac{\langle \tau_m \rangle}{\langle \tau_M \rangle^2} \left(1 - \frac{\langle \tau_m \rangle}{\langle \tau_M \rangle}\right) \left(A_{\Delta m} \frac{\tau_M}{\langle \tau_M \rangle} + 1\right) \\ \times e^{-\frac{\tau_M - \sum_{i=1}^n \tau_m^{(i)}}{\langle \tau_M \rangle}} \prod_{i=1}^n \left\{ 1 - \left(\frac{\tau_m^{(i)} - \frac{\langle \tau_M \rangle}{A_{\Delta m}}}{\tau_M + \frac{\langle \tau_M \rangle}{A_{\Delta m}}} \right) \right\}. \quad (40)$$

175 Note that functions (36)–(40) do not satisfy the normalization condition. Further-
 176 more, in some cases, $p_{Mm}^{\text{approx}}(\tau_M|\tau_m^{(1)}, \dots, \tau_m^{(n)})$ in Equations (36) and (39) may take neg-
 177 ative values when the correction term is larger than the kernel part. The relationship
 178 between the inverse probability density function and its approximation function is dis-
 179 cussed in Appendix G.

180 5 Examination of Bayesian updating method in uncorrelated time se- 181 ries

182 In this section, we compute the inverse probability density function given by Equa-
 183 tion (24) and the (part of) approximation function (Equations (36)–(40)) for the numer-
 184 ically generated uncorrelated time series, and we compare their properties (Tanaka &
 185 Umeno, 2021). We examine the numerical method of the Bayesian updating by chang-
 186 ing some conditions to see its utility.

187 5.1 Time series generation and Bayesian updating methods

188 The uncorrelated time series can be numerically generated by setting $\lambda(t) \equiv \lambda_0$
 189 in Equation (1). In fact, it is numerically generated as the renewal process in which mag-
 190 nitudes and time intervals are generated randomly obeying Equations (9) and (10), re-
 191 spectively. We set the parameter values to be $b = 1$ and $\lambda_0 = 0.0007$. The magnitude
 192 thresholds are set to $(M, m) = (5.0, 3.0)$. The b -value condition of Equation (25) is sat-
 193 isfied for these settings. The occurrence time of each event is recorded to 20 decimal places.
 194 For such time series, Bayesian updating is applied as explained below.

195 Bayesian updating is executed for each lower interval in the order of appearance
 196 starting from the one immediately after the event with a magnitude above M by sub-
 197 stituting their lengths $\{\tau_m^{(1)}, \tau_m^{(2)}, \dots, \tau_m^{(n)}\}$ into Equations (24), (39), and (40). The sum-
 198 mation of the lower intervals at the n -th update $\sum_{i=1}^n \tau_m^{(i)}$ is equivalent to the elapsed
 199 time T from the previous event with a magnitude above M . Further, the updating is per-
 200 formed until the event immediately before the next large event with a magnitude above
 201 M (i.e., the rightmost lower interval in an upper interval is not used). Therefore, we con-
 202 sider only cases where at least one event is (or two lower intervals are) included in an
 203 upper interval.

204 In addition, we use the following numerical method based on Equations (36) and
 205 (37). First, we generate \mathcal{N} time series each contains 10^5 events as sample data. From
 206 these sample data, numerically obtain the statistics required for the calculating Equa-
 207 tions (36) and (37), i.e., $p_m(\tau_m)$, $p_M(\tau_M)$, $p_{mM}(\tau_m|\tau_M)$ and $P_i(\tau_m|\tau_M)$, and the aver-
 208 age number of lower intervals included in the upper interval of length τ_M , $\tau_M/\langle\langle\tau_m\rangle\rangle_{\tau_M}$.
 209 Although the last one is a quantity related to the conditional probability, we calculate
 210 it separately. Moreover, we calculate only $P_1(\tau_m|\tau_M)$ and use it instead of $P_i(\tau_m|\tau_M)$
 211 for $i \geq 2$.

These statistics are obtained as a vector or a matrix on discretized intervals as

$$\begin{aligned} \tau_{m,j} &:= 10^{(j+0.5)\Delta\tau_m}, \\ \tau_{M,k} &:= 10^{(k+0.5)\Delta\tau_M}, \end{aligned} \quad (41)$$

where $j, k \in \mathbb{Z}$, such that

$$\begin{aligned} \mathbf{p}_m &= [p_{m,j}]_{j=j_{\min}, \dots, j_{\max}}, \\ \mathbf{p}_M &= [p_{M,k}]_{k=k_{\min}, \dots, k_{\max}}, \\ \mathbf{p}_{mM} &= [p_{mM,jk}]_{j=j_{\min}^{(k)}, \dots, j_{\max}^{(k)}}_{k=k_{\min}, \dots, k_{\max}}, \\ \mathbf{P}_1 &= [P_{1,jk}]_{j=j_{\min}^{(k)}, \dots, j_{\max}^{(k)}}_{k=k_{\min}, \dots, k_{\max}}. \end{aligned} \quad (42)$$

212 In Equation (42), j_{\min} , j_{\max} , k_{\min} , and k_{\max} represent the smallest and largest bin num-
 213 bers of each distribution. For the statistics obtained as a matrix, the range of j depends
 214 on k , and this is indicated as $j_{\min}^{(k)}$ and $j_{\max}^{(k)}$. The ranges of j and k are different for dis-
 215 tribution; however, the same symbol is used in Equation (42). In this paper, we fix $\Delta\tau_m =$
 216 0.1, and in this section, we examine the cases $\mathcal{N} = 10^3, 10^5$ and $\Delta\tau_M = 0.1, 0.025$. In
 217 the case $\mathcal{N} = 10^5$, they are fully used only for $p_{mM}(\tau_m|\tau_M)$ and $P_1(\tau_m|\tau_M)$, and only
 218 10^3 of them are used for $p_m(\tau_m)$, $p_M(\tau_M)$, and $\tau_M/\langle\langle\tau_m\rangle\rangle_{\tau_M}$.

219 To use these amounts in numerical Bayesian updating, we perform the following
 220 interpolations between the data points and extrapolations outside the data range. We
 221 describe these procedures using the example of the case $\mathcal{N} = 10^3$ and $\Delta\tau_M = 0.1$.

222 First, for the inter-event time distributions (\mathbf{p}_m and \mathbf{p}_M), we interpolate between
 223 the data points of each distribution (between $\tau_{m,j}$ and $\tau_{M,k}$, respectively) using cubic
 224 spline functions. Outside the data range (i.e., $\tau_m < \tau_{m,j_{\min}}$, $\tau_m > \tau_{m,j_{\max}}$ and $\tau_M <$
 225 $\tau_{M,k_{\min}}$, $\tau_M > \tau_{M,k_{\max}}$), we extrapolate the fitting curve for the edge 10 points (Fig-
 226 ure S1). The distributions are defined for all continuous τ_m values and for all $\tau_{M,k}$ us-
 227 ing this process.

228 Second, for the bivariate distributions (\mathbf{p}_{mM} and \mathbf{P}_1), we perform the same inter-
 229 polations and extrapolations for $\tau_{m,j}$ (Figures S2 and S3). Meanwhile, for $\tau_{M,k}$, the do-
 230 main is extended using the average of the functions at $\{\tau_{M,k_{\min}}, \dots, \tau_{M,k_{\min}+l_e-1}\}$ as the
 231 substitute for $\tau_{M,k}$ with $k < k_{\min}$, whereas using the functions at $\{\tau_{M,k_{\max}-l_e+1}, \dots, \tau_{M,k_{\max}}\}$
 232 as the substitute for $\tau_{M,k}$ with $k > k_{\max}$. We set $l_e = 5$ for $\Delta\tau_M = 0.1$ and $l_e = 20$
 233 for $\Delta\tau_M = 0.025$.

234 Finally, for $\tau_{M,k}/\langle\langle\tau_m\rangle\rangle_{\tau_{M,k}}$, the interpolation and extrapolation procedures are con-
 235 ducted in the same way as \mathbf{p}_M , although the extrapolation functions are different (Fig-
 236 ure S4).

237 Thus, the discrete variable $\tau_{m,j}$ becomes continuous as τ_m and the distribution func-
 238 tions are defined for all τ_m larger than 0. This makes it possible to return a value for
 239 any input of the length of a lower interval when performing Bayesian updating. Further,
 240 the distribution functions are defined for any k in Equation (41). We set the range of
 241 k to be $-120 \leq k \leq 70$ for $\Delta\tau_M = 0.1$, and $-480 \leq k \leq 280$ for $\Delta\tau_M = 0.025$. Al-
 242 though this yields the maximum range of the Bayesian updating, the updating at the
 243 n -th step is performed within the range $\max\{\tau_m^{(1)}, \dots, \tau_m^{(n)}\} < \tau_M$. The properties of
 244 the inverse probability density function and the (part of) approximation function are ex-
 245 amined within this range.

The kernel parts of the approximation functions are computed by calculating Equa-
 tion (37) in a step-by-step manner as

$$\begin{aligned}
 \ln p_{Mm}^{\text{kernel}}(\tau_{M,k}|\tau_m^{(1)}) &= \ln \left(\frac{\langle\tau_m\rangle}{\langle\tau_M\rangle} \frac{\tau_{M,k}}{\langle\langle\tau_m\rangle\rangle_{\tau_{M,k}}} \right) + \ln p_{mM}(\tau_m^{(1)}|\tau_{M,k}) - \ln p_m(\tau_m^{(1)}) + \ln p_{M,k}, \\
 \ln p_{Mm}^{\text{kernel}}(\tau_{M,k}|\tau_m^{(1)}, \tau_m^{(2)}) &= -\ln \left(1 - \frac{\langle\tau_m\rangle}{\langle\tau_M\rangle} \right) + \ln p_{mM}(\tau_m^{(2)}|\tau_{M,k}) - \ln p_m(\tau_m^{(2)}) + \ln p_{Mm}^{\text{kernel}}(\tau_{M,k}|\tau_m^{(1)}), \\
 \ln p_{Mm}^{\text{kernel}}(\tau_{M,k}|\tau_m^{(1)}, \tau_m^{(2)}, \tau_m^{(3)}) &= -\ln \left(1 - \frac{\langle\tau_m\rangle}{\langle\tau_M\rangle} \right) + \ln p_{mM}(\tau_m^{(3)}|\tau_{M,k}) - \ln p_m(\tau_m^{(3)}) + \ln p_{Mm}^{\text{kernel}}(\tau_{M,k}|\tau_m^{(1)}, \tau_m^{(2)}), \\
 &\vdots
 \end{aligned} \tag{43}$$

The correction terms of the approximation functions are calculated by first update as

$$\begin{aligned}
 \ln p_{Mm}^{\text{correct}}(\tau_{M,k}|\tau_m^{(1)}) &= \ln \left(\frac{\langle \tau_m \rangle}{\langle \tau_M \rangle} \right) + \ln P_1(\tau_m^{(1)}|\tau_{M,k}) - \ln p_m(\tau_m^{(1)}) + \ln p_{M,k}, \\
 \ln p_{Mm}^{\text{correct}}(\tau_{M,k}|\tau_m^{(1)}, \tau_m^{(2)}) &= -\ln \left(1 - \frac{\langle \tau_m \rangle}{\langle \tau_M \rangle} \right) + \ln P_1(\tau_m^{(2)}|\tau_{M,k}) - \ln p_m(\tau_m^{(2)}) + \ln p_{Mm}^{\text{correct}}(\tau_{M,k}|\tau_m^{(1)}), \\
 \ln p_{Mm}^{\text{correct}}(\tau_{M,k}|\tau_m^{(1)}, \tau_m^{(2)}, \tau_m^{(3)}) &= -\ln \left(1 - \frac{\langle \tau_m \rangle}{\langle \tau_M \rangle} \right) + \ln P_1(\tau_m^{(3)}|\tau_{M,k}) - \ln p_m(\tau_m^{(3)}) + \ln p_{Mm}^{\text{correct}}(\tau_{M,k}|\tau_m^{(1)}, \tau_m^{(2)}), \\
 &\vdots
 \end{aligned} \tag{44}$$

and then, we add $\ln(n-1)$ for each $\ln p_{Mm}^{\text{correct}}(\tau_M|\tau_m^{(1)}, \dots, \tau_m^{(n)})$.

The approximation functions are obtained by adding together the kernel part and the correction term calculated by these separate updates. The approximation functions are calculated only for such k 's that $p_{\text{sup}} > \ln p_{Mm}^{\text{kernel}}, \ln p_{Mm}^{\text{correct}} > p_{\text{inf}}$. Here, $p_{\text{sup}} (= 600)$ and $p_{\text{inf}} (= -600)$ yield the upper and lower limits of p_{Mm}^{kernel} and p_{Mm}^{correct} to ensure that these are within the range of the computer capacity. In addition, such k 's for which the correction term is so large that Equation (36) becomes negative are excluded.

Figure S5 shows an example of Bayesian updating for the uncorrelated time series. The inverse probability density function given by Equation (24) has a characteristic peak that is not observed in $p_M(\tau_M)$. The correction term makes the kernel part obtained from Equation (40) closer to the inverse probability density function. Moreover, the numerical calculations based on Equations (36) and (37) with $\mathcal{N} = 10^3$ and $\Delta\tau_M = 0.1$ appear to be consistent with these results.

In the next subsection, we compare these functions statistically to examine numerical Bayesian updating method.

5.2 Examination of numerical Bayesian updating method

In this subsection, we compare the probability density functions and the (part of) approximation functions statistically. The Bayesian updating method described in the previous subsection is applied to 100 test data time series, each containing 10^5 events prepared separately from the sample data.

5.2.1 Comparison by distance

We define the distance for two square-integrable functions $f(\cdot)$ and $g(\cdot)$ as

$$D(f||g) := \int_T^\infty |f(\tau_M) - g(\tau_M)|^2 d\tau_M. \tag{45}$$

The range of the integral is set to (T, ∞) to exclude the Dirac's delta function at $\tau_M = T$ in the inverse probability density function. For $f = p_{Mm}(\tau_M|\tau_m^{(1)}, \dots, \tau_m^{(n)})$ and $g = p_M(\tau_M)$, the distance can be analytically derived (Appendix H), whereas when $f(\cdot)$ or $g(\cdot)$ is the (part of) approximation function, the distance is calculated numerically as

$$D(f||g) \simeq \sum_{\substack{k; \tau_{M,k} > T \\ p_{\text{sup}} > \ln f, \ln g > p_{\text{inf}}}} |f(\tau_{M,k}) - g(\tau_{M,k})|^2 (\ln 10) \tau_{M,k} \Delta\tau_M. \tag{46}$$

$D(f||g)$ is calculated for each update throughout the 100 test data time series. If no k 's satisfy $p_{\text{sup}} > \ln f, \ln g > p_{\text{inf}}$, it is not included in the following calculation. The average distance $\langle D(f||g) \rangle$ is calculated by averaging these distances for each elapsed time $T \in [10^{0.1l}, 10^{0.1(l+1)})$ with $l \in \mathbb{Z}$ from the previous event larger than M .

271 Figure 7(a) shows the average distance for the cases $f = p_{Mm}(\tau_M|\tau_m^{(1)}, \dots, \tau_m^{(n)})$,
 272 $p_{Mm}^{\text{approx}}(\tau_M|\tau_m^{(1)}, \dots, \tau_m^{(n)})$, $p_{Mm}^{\text{kernel}}(\tau_M|\tau_m^{(1)}, \dots, \tau_m^{(n)})$, and $g = p_M(\tau_M)$. In addition to
 273 the analytical calculation in Equation (45) for $D(p_{Mm}||p_M)$, the results of the numer-
 274 ical integration of Equation (46) are presented; the calculations using Equations (39) and
 275 (40) are indicated by $D'(\cdot||\cdot)$. The results of the calculation using Equations (36) and
 276 (37) with the numerical method in §5.1 with $\mathcal{N} = 10^3$ and $\Delta\tau_M = 0.1$ are presented
 277 by $D''(\cdot||\cdot)$. The results for $\mathcal{N} = 10^5$ with $\Delta\tau_M = 0.1$ and $\Delta\tau_M = 0.025$ are shown in
 278 Figure S6.

279 First, one can see that $\langle D'(p_{Mm}||p_M) \rangle$ is almost consistent with $\langle D'(p_{Mm}^{\text{approx}}||p_M) \rangle$,
 280 which indicates that $p_{Mm}^{\text{approx}}(\tau_M|\tau_m^{(1)}, \dots, \tau_m^{(n)})$ derived in the previous section certainly
 281 approximates the inverse probability density function, regardless of the elapsed time (or
 282 regardless of the number of updates, because the occurrence rate is constant). However,
 283 these separate from $D(p_{Mm}||p_M)$ at around $T \sim 10^5$ and at a large T . As such separa-
 284 tions disappear when $\Delta\tau_M = 0.025$ (Figure S6(c,d)), this is attributed to the coarse-
 285 ness of the numerical integration.

286 Second, $\langle D'(p_{Mm}^{\text{kernel}}||p_M) \rangle$ is nearly consistent with $\langle D''(p_{Mm}^{\text{kernel}}||p_M) \rangle$. This suggests
 287 that the numerical updating method in Equation (43) certainly calculates the kernel part.
 288 However, $\langle D''(p_{Mm}^{\text{approx}}||p_M) \rangle$ gradually separates from $\langle D'(p_{Mm}^{\text{approx}}||p_M) \rangle$ at a large T . This
 289 separation is more clearly illustrated in Figure 7(b), which shows the average distances
 290 between $f = p_{Mm}^{\text{approx}}, p_{Mm}^{\text{kernel}}$ and $g = p_{Mm}$ calculated by Equation (46). This separa-
 291 tion can be attributed to the calculation of the correction term in Equation (44), in par-
 292 ticular to the fluctuation in the numerically obtained \mathbf{P}_1 (Appendix I).

293 5.2.2 Comparison by maximum peak time

294 In the previous subsection, the approximation function calculated by the numer-
 295 ical Bayesian updating method is suggested to be separate from the inverse probability
 296 density function. However, we show that such a separation does not have a considerable
 297 effect around the maximum peak. To this end, we further compare the maximum points
 298 (hereafter, maximum peak time) of the inverse probability density function in Equation
 299 (23) and its approximation function in Equation (36) with the numerical updating method,
 300 each denoted by $\hat{\tau}_M^{\text{max}}$ and $\tau_M^{\text{max,approx}}$. Both functions are discretized as Equation (41);
 301 the corresponding k in Equation (41) is denoted by \hat{k}^{max} and $k^{\text{max,approx}}$, respectively.

302 \hat{k}^{max} and $k^{\text{max,approx}}$ are numerically searched for each update. These are deter-
 303 mined as such k that the function takes the maximum value within the range for which
 304 the above mentioned numerical results are obtained, while excluding its edges. Thus, if
 305 \hat{k}^{max} or $k^{\text{max,approx}}$ is located at such edges, it is not considered the peak and is set to
 306 $k = 80$ when $\Delta\tau_M = 0.1$ and $k = 320$ when $\Delta\tau_M = 0.025$. Further, when the numeri-
 307 cal results of the approximation function are not obtained for any k (when the correc-
 308 tion term exceeds the kernel part for all k), $k^{\text{max,approx}}$ is set to be 80 or 320.

309 Figure 8 shows the joint probability mass function (p.m.f.) of $(\hat{k}^{\text{max}}, k^{\text{max,approx}})$
 310 for $\mathcal{N} = 10^3$ and $\Delta\tau_M = 0.1$. Those for $\mathcal{N} = 10^5$ are presented in Figure S7. Here,
 311 the population is all the pairs of $(\hat{k}^{\text{max}}, k^{\text{max,approx}})$ obtained for each update through-
 312 out the test data. The maximum peak search is conducted in the two ranges; (a) $\tau_M >$
 313 $\max\{\tau_m^{(1)}, \dots, \tau_m^{(n)}\}$, and (b) $\tau_M > T$. In the former case, the p.m.f. is bimodal; the
 314 higher peak exists around $\hat{k}^{\text{max}} = k^{\text{max,approx}}$, and the other lower peak around $\hat{k}^{\text{max}} >$
 315 $k^{\text{max,approx}}$. The second peak disappears in the latter case, and the first peak is intrin-
 316 sic, i.e., the positions of the maximum peak are close between the inverse probability den-
 317 sity function and its approximation function. The situation is the same for other cases
 318 (Figure S7). These results indicate that it is the off-peak region of the approximation
 319 function that contributes to the separation of the average distances.

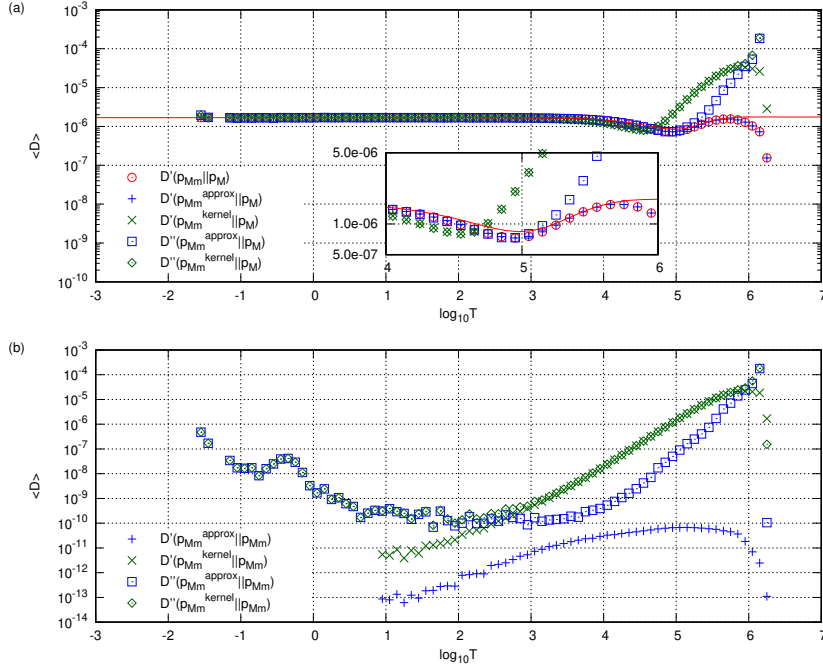


Figure 7. Average distances for each elapsed time (T) from the previous large event with a magnitude above M . (a) Distances between the inter-event time distribution and other function. $D(p_{Mm} || p_M)$ (Equation (H2) in Appendix H) is shown by the red curve, and the symbols are numerical results for Equation (46). (b) Distances between the inverse probability density function and other function numerically calculated by Equation (46).

320 The results obtained in this section indicate that the numerical method using 1100
 321 time series (1000 for sample data and 100 for test data) is sufficient to calculate the ker-
 322 nel part as well as the maximum peak time of the approximation function that is imp-
 323 portant in the inference, and to examine their statistical property. Further, these results
 324 indicate that Bayesian updating can be applied with the numerical method even if the
 325 explicit functional forms of the inter-event time distribution and the conditional prob-
 326 ability density function and so on are unclear, such as the time series of the ETAS model.

327 6 Bayesian updating for the time series of the ETAS model

328 In this section, Bayesian updating is applied to the time series of the ETAS model
 329 (Tanaka & Umeno, 2021). In this case, due to the correlations among events, it is dif-
 330 ficult to derive the inverse probability density function and its approximation function
 331 analytically. Therefore, we compute the approximation function (Equation (36)) and its
 332 kernel part (Equation (37)) using the numerical Bayesian updating method. The max-
 333 imum peak time of the kernel part is used as the estimate for the occurrence time of the
 334 next large event, and the effectiveness of forecasting based on that estimate is evaluated
 335 statistically.

336 6.1 Time series generation and Bayesian updating methods

337 We apply the numerical Bayesian updating method in §5.1 to the time series gener-
 338 ated by Equation (1) with the parameter values $b = 1$, $\alpha = 0.8$, $\theta = 0.2$ ($p = 1.2$),
 339 $c = 0.01$, $M_0 = 3$, $\lambda_0 = 0.0007$, and $K = 0.0125$. The magnitude thresholds are

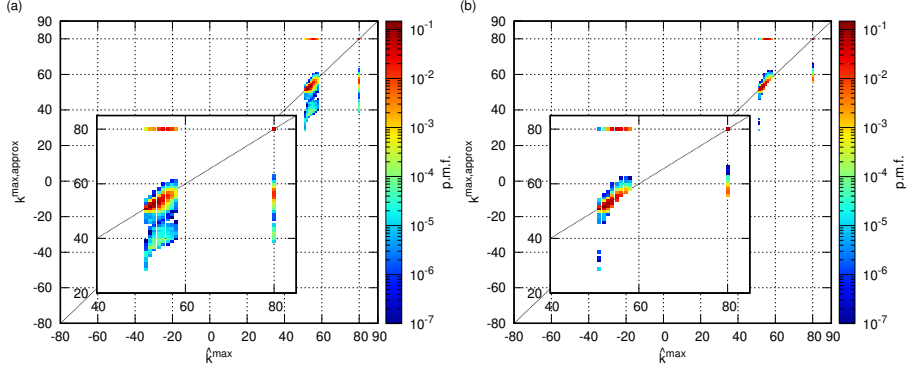


Figure 8. Joint probability mass function for $(\hat{k}^{\max}, k^{\max, \text{approx}})$. Numerical search of the maximum peak is conducted for (a) $\tau_M > \max\{\tau_m^{(1)}, \dots, \tau_m^{(n)}\}$ and (b) $\tau_M > T$. The horizontal line at $k^{\max, \text{approx}} = 80$ and the vertical line at $\hat{k}^{\max} = 80$ correspond to the cases when the peak is not detected by the peak search.

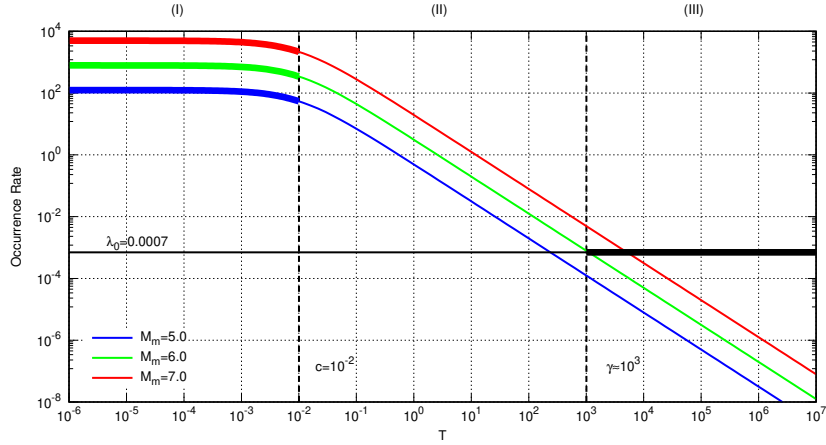


Figure 9. Omori-Utsu law for the parameter values in the text with a different mainshock magnitude M_m . The number of aftershocks per unit day against the elapsed time (T) from the mainshock obeys $\lambda(T) = K10^{\alpha(M_m - M_0)} / (T + c)^{\theta+1}$. The background rate ($\lambda_0 = 0.0007$) is also shown.

340 $(M, m) = (5.0, 3.0)$. Although the entire time series is stationary because the branch-
 341 ing ratio ($n_{\text{br}} \approx 0.785$) is less than 1, it is locally non-stationary obeying the Omori-Utsu
 342 law after a large event, as shown in Figure 9. The activity can be categorized into three
 343 regimes with respect to the elapsed time (T) from the mainshock, as summarized in Ta-
 344 ble 1.

345 We prepare 1100 time series, with each containing 10^5 events. First, random num-
 346 bers generated from five different seed values are used to generate 240 time series for each
 347 seed. Among them, those contain events with magnitude above 10 are excluded. This
 348 is because the aftershock sequence excited by such an unrealistic large event do not fit
 349 within a single time series, and then, the non-stationarity affects the statistics of the sam-
 350 ple data. We use 1100 of the remaining time series. $\mathcal{N} = 1000$ are used as the sample
 351 data to obtain statistics with $\Delta\tau_M = 0.1$; the interpolation and extrapolation proce-
 352 dures are conducted with $l_e = 5$ in the same way as explained in §5.1 (Figures S8-S12).
 353 Bayesian updating (Equations (43) and (44)) is applied to the remaining 100 time se-

Table 1. *Three Regimes in the time series of the ETAS model*

Category	Regime	Property
(I)	$T \lesssim c (= 0.01)$	Stationary, high occurrence rate
(II)	$c \lesssim T \lesssim \gamma (\approx 10^3)$	Non-stationary, relaxation process
(III)	$\gamma \lesssim T$	Stationary, low occurrence rate ($\lesssim \lambda_0$)

354 ries. The maximum range of k is $-120 \leq k \leq 70$, and the n -th update from the
 355 occurrence time of the event above M is conducted in the range $\max\{\tau_m^{(1)}, \dots, \tau_m^{(n)}\} < \tau_M$.
 356 The numerical update is conducted when the lower interval is above 0 (for the occur-
 357 rence times recorded to 20 decimal places); otherwise, the update is skipped.

The following normalizations are performed in the calculations of the Bayesian updating. The result of the calculation in Equation (43) can be very large. In order to compute the approximation functions together with Equation (44), it is necessary to use the function value of p_{Mm}^{kernel} as it is, though it can exceed p_{sup} . Therefore, to avoid such enlargement, we normalize the result of Equation (43) for each update by subtracting the following numerical integration from Equation (43).

$$\ln \left(\sum_{\substack{k; \tau_{M,k} > T \\ p_{\text{sup}} > \ln p_{Mm}^{\text{kernel}} > p_{\text{inf}}}} p_{Mm}^{\text{kernel}}(\tau_{M,k} | \tau_m^{(1)}, \dots, \tau_m^{(n)}) (\ln 10) \tau_{M,k} \Delta \tau_M \right). \quad (47)$$

358 Further, it is necessary to subtract Equation (47) from the correction term in Equation
 359 (44) at the same time (thereby the entire approximation function is multiplied by a con-
 360 stant). Thus, for each update of Equations (43) and (44), the numerical integration (47)
 361 is computed and subtracted from both.

362 6.2 Comparison of the approximation function and its kernel part

363 It is difficult to obtain $P_i(\tau_m | \tau_M)$ for the ETAS model, and therefore, we exam-
 364 ine the contribution from the correction term to the approximation function as follows.
 365 Instead of $P_i(\tau_m | \tau_M)$, we calculate the probability density functions $P^L(\tau_m | \tau_M)$ and $P^R(\tau_m | \tau_M)$
 366 (Figures S10 and S11). According to the Omori–Utsu law, we consider that these two
 367 are the end-members of $P_i(\tau_m | \tau_M)$. Then, the approximation functions are calculated
 368 numerically by replacing all $P_i(\tau_m | \tau_M)$'s in Equation (44) by either $P^L(\tau_m | \tau_M)$ or $P^R(\tau_m | \tau_M)$.
 369 We denote the maximum peak times of these approximation functions by $\tau_M^{\text{max,L}}$ and $\tau_M^{\text{max,R}}$,
 370 and their corresponding k 's in Equation (41) by $k^{\text{max,L}}$ and $k^{\text{max,R}}$, respectively. Sim-
 371 ilarly, they are denoted by τ_M^{max} and k^{max} for the kernel part, hereafter. The numerical
 372 search of $k^{\text{max,L}}$, $k^{\text{max,R}}$, and k^{max} is conducted in the same way as indicated in §5.2 in
 373 the range $\tau_M > \max\{\tau_m^{(1)}, \dots, \tau_m^{(n)}\}$.

374 Figure 10 shows the joint p.m.f. of $(k^{\text{max}}, k^{\text{max,L}})$ and $(k^{\text{max}}, k^{\text{max,R}})$, which is cal-
 375 culated in the same way as indicated in §5.2. The maximum peak time of the kernel part
 376 is not significantly affected by the correction term, and then, it can be used to infer that
 377 of the inverse probability density function. However, its confidence interval or average
 378 cannot be used because the correction term is not taken into account. In the following,
 379 we use the maximum peak time of the kernel part (τ_M^{max}) as the estimator of the occur-
 380 rence time of the next large event with a magnitude above M , and we discuss the effec-
 381 tiveness of the forecasting based on the estimates.

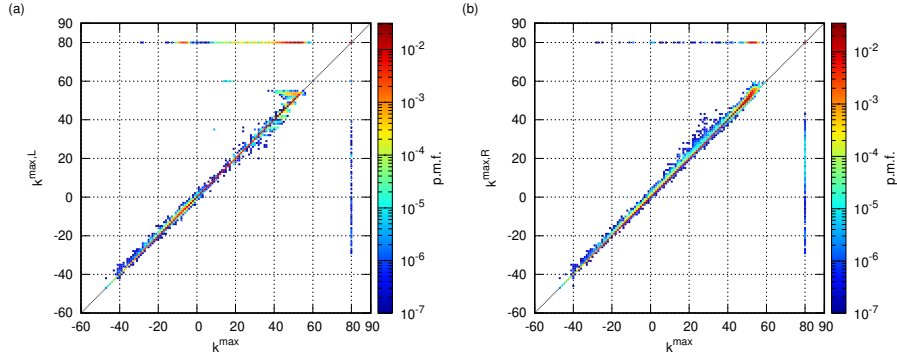


Figure 10. Joint probability mass functions for (a) $(k^{\max}, k^{\max,L})$ and (b) $(k^{\max}, k^{\max,R})$. The horizontal lines at $k^{\max,L} = 80$ and $k^{\max,R} = 80$ and the vertical line $k^{\max} = 80$ are the cases where the peak is not detected.

382
383

6.3 Estimation of the occurrence time of the next large event and effectiveness of forecasting

We denote the estimate at the n -th update by $\tau_M^{\max,n} (= 10^{(k^{\max,n}+0.5)\Delta\tau_M})$, and the actual elapsed time of the next large event from the previous one by τ_M^* . We evaluate the accuracy of the estimation at the n -th update using the relative error (δ_n), which is given as

$$\delta_n := \frac{\tau_M^* - \tau_M^{\max,n}}{\tau_M^*}, \quad (48)$$

384
385
386

Equation (48) considers that the error $|\tau_M^* - \tau_M^{\max,n}|$ gets larger as τ_M^* becomes longer. The relative error makes it possible to evaluate the accuracy in a manner that is comparable regardless of τ_M^* .

The accuracy at the n -th update is judged by whether δ_n is within the threshold (δ_{th})

$$-\delta_{\text{th}} \leq \delta_n \leq \delta_{\text{th}}. \quad (49)$$

When Equation (49) is satisfied, the estimation at the n -th update is judged to be plausible for the given threshold value δ_{th} in the present paper. This is equivalent for the actual occurrence time to be within the range

$$\frac{\tau_M^{\max,n}}{(1 + \delta_{\text{th}})} \leq \tau_M^* \leq \frac{\tau_M^{\max,n}}{(1 - \delta_{\text{th}})}. \quad (50)$$

387
388
389
390
391
392
393
394
395
396

Based on the above accuracy at each update, we further evaluate whether a series of estimations yields effective forecasting. Here, effective forecasting implies that τ_M^{\max} takes a nearly constant value around τ_M^* continuously from well before the occurrence time of the next large event. This can be quantitatively expressed as follows: Let $n_{\leq \text{th}}$ be the number of consecutive updates immediately before the next large event, in which Equation (49) is satisfied. Further, we denote the last update as the n_{fin} -th update. When the sequence of updates with a sufficiently long $n_{\leq \text{th}}$ exists in the range of $n \in (n_{\text{fin}} - n_{\leq \text{th}}, n_{\text{fin}}]$, we consider the forecasting to be effective. We judge the stability of $\tau_M^{\max,n}$ by Equation (49), and therefore, δ_{th} should not be too large. In the present paper, we set $\delta_{\text{th}} = 0.5$ and 0.25 .

To observe the relationship between the effectiveness of forecasting and the stationarity of the time series, we examine the occurrence rate (R_n), variation of its log ($\Delta \log_{10} R_n$), and variation of log-estimate (Δk_n^{\max}) defined below.

$$R_n := 10 / (t_{n+9} - t_n), \quad (51)$$

$$\Delta \log_{10} R_n := \log_{10} R_{n+10} - \log_{10} R_n, \quad (52)$$

$$\Delta k_n^{\max} := k^{\max, n+10} - k^{\max, n}, \quad (53)$$

397 where t_n represents the occurrence time of the n -th update.

398 Figures S11–S13 show examples of Bayesian updating for each regime in Table 1.
 399 Although these are only examples and not all updating proceeds in this way, these ex-
 400 amples suggest that the stability of the estimate is related to the stationarity of the time
 401 series.

402 6.4 Statistical analysis of the effectiveness of forecasting

403 We show the results of the statistical analysis on the effectiveness of forecasting.
 404 Only the cases of $n_{\text{fin}} \geq 30$ are used in the analysis to ensure that the temporal infor-
 405 mation of lower intervals is fully reflected in the estimate. Figure 11(a) shows the total
 406 number of upper intervals (N) obtained from the test data for each $\tau_M^* \in [10^{0.5l}, 10^{0.5(l+1)})$
 407 with $l \in \mathbb{Z}$. Further, N_{30} represents the total number of upper intervals such that $n_{\text{fin}} \geq$
 408 30 , which is shown with the ratio to N . The updates included in these N_{30} upper inter-
 409 vals are analyzed.

410 Figures 11(b–d) show the results of the statistical analysis with $\delta_{\text{th}} = 0.5$. Fig-
 411 ure 11(b) shows the probability (P_{fin}) of $n_{\leq \text{th}} > 0$ (or $|\delta_{n_{\text{fin}}}| \leq \delta_{\text{th}}$) for each τ_M^* . The
 412 average of P_{fin} for the overall τ_M^* is about 0.52, and the P_{fin} for each τ_M^* is about the same,
 413 except for $\tau_M^* > \langle \tau_M \rangle$ in which P_{fin} takes a higher probability around 0.67. Of such $n_{\leq \text{th}} >$
 414 0 cases, the proportion ($P_{\geq 30}$) of those with relatively long $n_{\leq \text{th}} \geq 30$ is also shown in
 415 Figure 11(b) (the probability distribution of $n_{\leq \text{th}}$ is shown in Figure S16(a)). Thus the
 416 regions of high $P_{\geq 30}$ are overlapped with regimes (I) and (III), though the former is shifted
 417 toward larger τ_M^* . On the other hand, $P_{\geq 30}$ is lower in regime (II); it gradually decreases
 418 as τ_M^* gets larger. This is consistent with the average of $n_{\leq \text{th}}$ ($\langle n_{\leq \text{th}} \rangle$, this average is taken
 419 for $n_{\leq \text{th}} > 0$), but also with the average of its proportion to n_{fin} ($\langle n_{\leq \text{th}} / n_{\text{fin}} \rangle$) as shown
 420 in Figure 11(c). This implies that, as the fraction of non-stationary times in $[0, \tau_M^*)$ in-
 421 creases in regime (II), the domination rate of $n_{\leq \text{th}}$ in the total n_{fin} -updates decreases grad-
 422 ually. These properties are preserved for $\delta_{\text{th}} = 0.25$ (Figure S17).

423 Figure 12 shows the joint probability density-mass functions of $\Delta \log_{10} R$ and Δk^{\max}
 424 calculated numerically for each τ_M^* . The case $k^{\max} = 80$ is excluded from the popula-
 425 tion. If τ_M^* is in the regions of high $P_{\geq 30}$, the distribution is almost symmetrically con-
 426 centrated near the origin. This implies that, when the time series is dominated by sta-
 427 tionarity ($\Delta \log_{10} R \approx 0$), the estimated value is stable ($\Delta k^{\max} \approx 0$). On the other
 428 hand, if τ_M^* is in regime (II), the probability density function gradually has a region in
 429 the second quadrant as τ_M^* gets larger. This region indicates the existence of a non-stationary
 430 time series in which the estimate has an increasing trend ($\Delta k^{\max} > 0$).

431 These results present the following conclusions. First, the probability that the rela-
 432 tive error is within the threshold at the last update ($|\delta_{n_{\text{fin}}}| \leq \delta_{\text{th}}$) is almost indepen-
 433 dent of the actual occurrence time (τ_M^*). This suggests that the length of the upper inter-
 434 val can be estimated by the inverse probability density function reflecting the tempo-
 435 ral pattern of lower intervals, at the last update when the information of the lower in-
 436 tervals can be utilized fully. Second, the stationarity of the time series is related to the
 437 stability of the estimate; if the time series is non-stationary, it causes the estimate τ_M^{\max}
 438 to shift. Third, the domination rate of stationarity in the time series determines the ef-
 439 fectiveness of forecasting. Immediately or long after the large event, the stationary time

440 series is dominant. Therefore, based on the second point mentioned above, the estimate
 441 becomes stable, which leads to an effective forecasting with a relatively long $n_{\leq \text{th}}$. How-
 442 ever, these regions are not identical to regimes (I) and (III). This is attributed to lag un-
 443 til the ratio of the non-stationary region in the time series becomes dominant. On the
 444 other hand, in regime (II), the non-stationarity becomes gradually dominant, which leads
 445 to the shifting of τ_M^{max} and shortening of $n_{\leq \text{th}}$.

446 Finally, we discuss the effectiveness of forecasting in terms of the duration time ($\tau_{\leq \text{th}}$)
 447 during the $n_{\leq \text{th}}$ updates. Figure 11(d) shows the average of the duration time ($\langle \tau_{\leq \text{th}} \rangle$)
 448 and the average of its ratio to the actual occurrence time ($\langle \tau_{\leq \text{th}} / \tau_M^* \rangle$) for each τ_M^* (the
 449 probability distribution of $\tau_{\leq \text{th}}$ is shown in Figure S16(b)). Unlike $\langle n_{\leq \text{th}} \rangle$ in Figure 11(c),
 450 $\langle \tau_{\leq \text{th}} \rangle$ increases linearly as τ_M^* gets larger, and it is sufficiently long in regime (III). On
 451 the other hand, $\tau_{\leq \text{th}}$ is very short in regime (I); however, the ratio $\langle \tau_{\leq \text{th}} / \tau_M^* \rangle$ is high
 452 (nearly 0.7). Therefore, from the perspective of the time interval, the forecasting is also
 453 considered to be effective immediately or long after the large event.

454 7 Discussion and Conclusions

455 The Bayes' theorem and Bayesian updating on the inter-event times at different
 456 magnitude thresholds in a marked point process are considered. The analytical results
 457 for the uncorrelated time series are used to apply Bayesian updating to the time series
 458 of the ETAS model for examining its utility toward forecasting a large event using the
 459 temporal pattern of the smaller events.

460 First, the Bayes' theorem is considered for the general marked point process. The
 461 Bayes' theorem provides the relationship between the conditional and inverse probabili-
 462 ty density functions for the lengths of one upper interval and one lower interval. The
 463 inverse probability density function is represented by the generalized forms of the prob-
 464 ability density functions of the inter-event times and the conditional probability density
 465 function. This inverse probability density function is derived for the uncorrelated time
 466 series analytically, and the condition to have a peak is also found.

467 The Bayes' theorem is extended to Bayesian updating that yields the inverse prob-
 468 ability density function between the lengths of multiple consecutive lower intervals and
 469 the upper interval that includes them. Although the inverse probability density func-
 470 tion is different for the updating manner, we consider the updating without the restric-
 471 tion on the position of the lower intervals. For the uncorrelated time series, the inverse
 472 probability density function and its approximation function are derived, and the latter
 473 approximation is shown to be reasonable using the distances.

474 Bayesian updating is applied to the time series of the ETAS model. We numeri-
 475 cally analyze the approximation function and its kernel part. We use the maximum point
 476 of the kernel part as the estimate of the occurrence time of the next large event because
 477 the maximum peaks of these two functions are shown to not be different drastically. The
 478 accuracy of the estimation at each update is evaluated by the relative error with the ac-
 479 tual occurrence time of the next large event; the effectiveness of the forecasting through-
 480 out the series of updates is judged by the continuity of the plausible estimations prior
 481 to the large event.

482 Statistical analysis indicates that the accuracy of the estimation at the last update
 483 does not drastically depend on the occurrence time of the next large event. This sug-
 484 gests that the inverse probability density function can estimate the occurrence time of
 485 the next large event in response to the temporal pattern of minor events. However, the
 486 continuity of plausible estimation depends on the occurrence time of the next large event.
 487 This is because the dominance rate of the non-stationary time series in which the esti-
 488 mate becomes unstable varies with the elapsed time from the previous large event obey-
 489 ing the Omori–Utsu law. The stationarity is dominant either immediately after or long

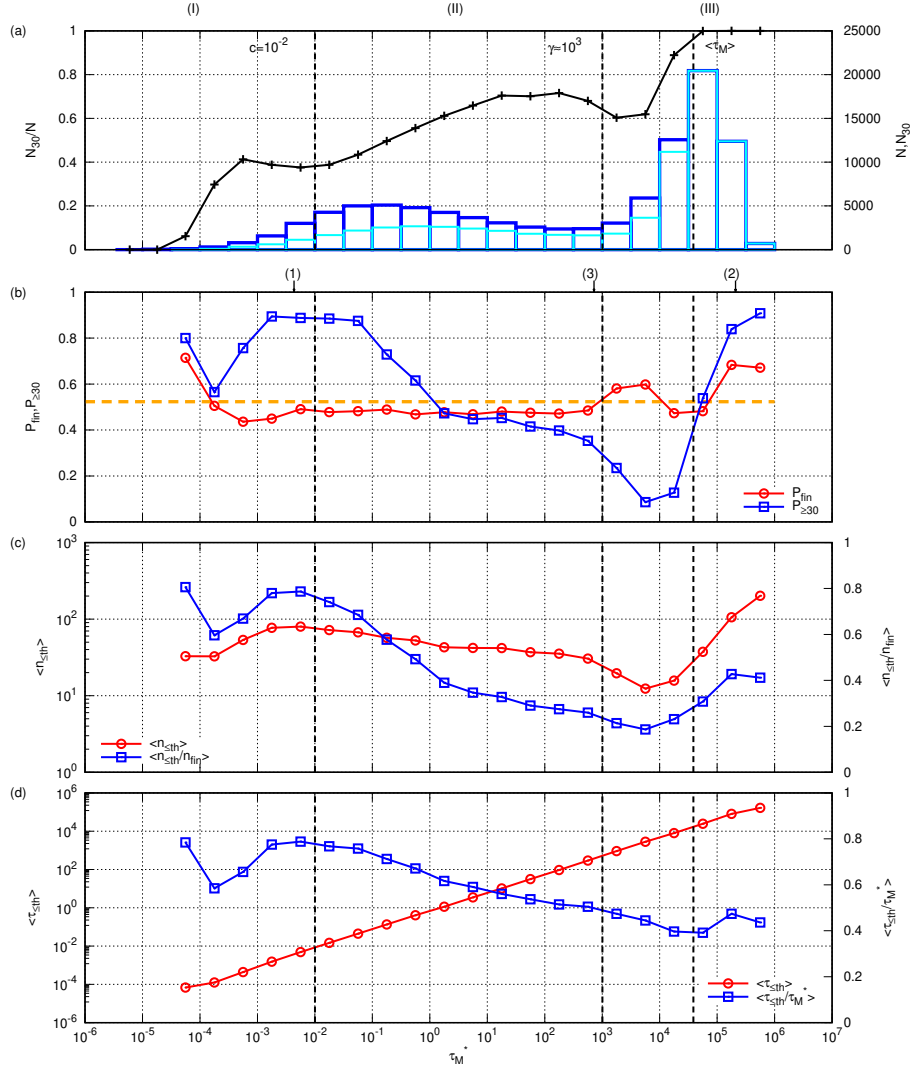


Figure 11. (a) (Blue) Number of upper intervals N , (Cyan) number of upper intervals that include at least 30 updates N_{30} , and (Black) their ratio N_{30}/N , for each τ_M^* in the test data. (b–d) Statistical results with $\delta_{\text{th}} = 0.5$ for each τ_M^* . (1)–(3) indicates the τ_M^* 's of the examples in Figures S13–S15. (b) (Red) Probability P_{fin} that $n_{\leq \text{th}} > 0$ holds (or the probability that Equation (49) is satisfied at the last $(n_{\text{fin}} - \text{th})$ update), and (Orange dotted line) the average of $P_{\text{fin}} \approx 0.52$ for the overall τ_M^* . (Blue) Proportion $P_{\geq 30}$ of such cases among them where $n_{\leq \text{th}} \geq 30$. (c) (Red) Average of $n_{\leq \text{th}}$, $\langle n_{\leq \text{th}} \rangle$, and (Blue) the average of its proportion to the total number of updates, $\langle n_{\leq \text{th}}/n_{\text{fin}} \rangle$. (d) (Red) Average of the duration time $\tau_{\leq \text{th}}$, $\langle \tau_{\leq \text{th}} \rangle$ and (Blue) the average of its proportion to the actual occurrence time, $\langle \tau_{\leq \text{th}}/\tau_M^* \rangle$.

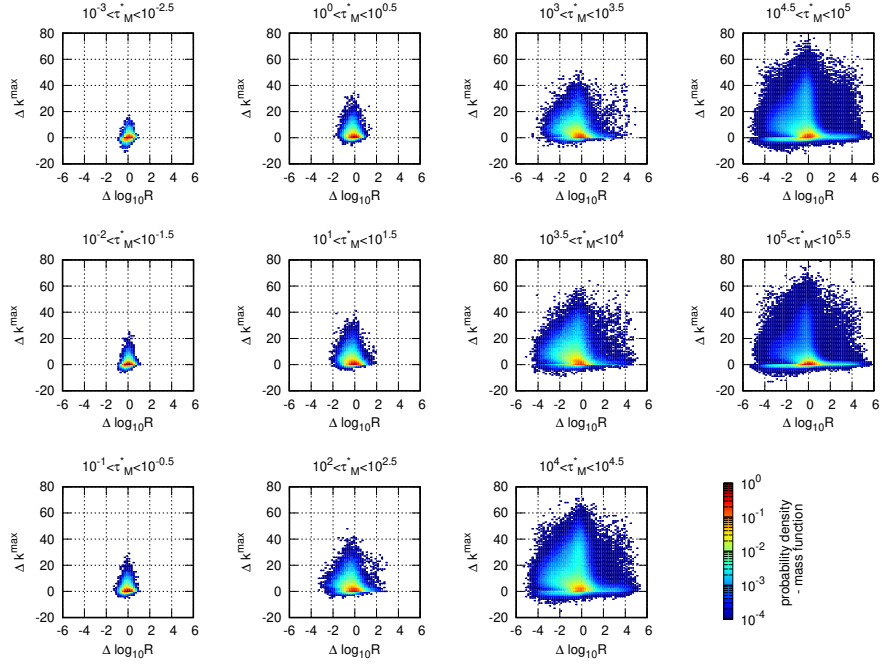


Figure 12. Joint probability density-mass functions of $\Delta \log_{10} R$ and Δk^{\max} for each τ_M^* .

490 after the previous major event. Therefore, the forecasting by the Bayesian updating method
 491 can be effective for secondary disaster prevention in the former case, and for long-term
 492 risk assessment in the latter case.

493 The approximation function derived for the uncorrelated time series is applied in
 494 the Bayesian updating for the time series of the ETAS model. This allows us to perform
 495 the update in the convenient form of the product of the conditional probabilities. How-
 496 ever, this implicitly assumes that there is no correlation between events and lower inter-
 497 vals; such an assumption can be reasonable for the stationary part of the time series,
 498 although it is not reasonable for non-stationary part. This probably is one of the reasons
 499 why forecasting is ineffective in the non-stationary regime.

500 Further, only the kernel part of the approximation function is used when estimat-
 501 ing the occurrence time of the next large event for the time series of the ETAS model.
 502 The correction term needs to be investigated in detail to use the entire approximation
 503 function to perform point estimation by average, interval estimation, or probabilistic risk
 504 assessment using hazard rate. Comparison with the probabilistic evaluation using the
 505 inter-event time distribution becomes possible after clarifying the correction term.

506 Although the statistical property of Bayesian updating is examined for only one
 507 set of ETAS parameters, it is considered to be different for activities generated by other
 508 parameter values. For example, for the time series with the high background rate (λ_0)
 509 that corresponds to taking up a large spatial area, forecasting is considered to be less
 510 effective because in such time series, different mainshock-aftershocks sequences overlap
 511 (Touati et al., 2009) and the correlations between the upper and lower intervals are weak-
 512 ened. Further, if the background rate is low, forecasting is considered to be improved
 513 because a single mainshock-aftershocks sequence is exposed (Touati et al., 2009) and the
 514 correlation is easily reflected in the conditional probability. Forecasting is also consid-
 515 ered to be improved for the time series with a large branching ratio (n_{br}). If the branch-
 516 ing ratio is large, the number of aftershocks generated by an event increases (Helmstetter

517 & Sornette, 2003), which increases the number of updates in the Bayesian updating; this
 518 is advantageous for forecasting.

519 In this study, only one lower threshold magnitude (m) is set for a given upper thresh-
 520 old (M). One approach for performing Bayesian updating using more temporal infor-
 521 mation of the lower intervals is to set multiple lower thresholds ($m_1 < m_2 < \dots (<$
 522 $M)$). When setting such lower thresholds, it is better to refer to the condition of $\Delta m >$
 523 $\log_{10} 3/b$ so that the inverse probability density function has a peak. This condition in-
 524 dicates that there is a trade-off between the b -value and Δm , and then, the range of lower
 525 thresholds that can be set varies with the b -value. However, the condition $\Delta m > \log_{10} 3/b$
 526 is for the uncorrelated time series; finding the corresponding condition for the time se-
 527 ries of the ETAS model is a future work. Considering such an extension is important for
 528 applying the Bayesian updating method to the real seismic catalogs in which the num-
 529 ber of earthquakes is limited.

530 To utilize as much temporal information on small events as possible using the method
 531 described above is important for applying the Bayesian updating method to real seis-
 532 mic catalogs with a limited number of data. Another idea to apply the Bayesian updat-
 533 ing method to seismic catalogs while compensating for the shortage of data is to use the
 534 ETAS model in combination. The ETAS model can be used to generate a sufficient amount
 535 of synthetic data with the parameter set determined for the past seismic activity. From
 536 such synthetic data, statistical amounts necessary in the numerical Bayesian updating
 537 method is obtained precisely. Moreover, it is necessary to develop further ingenuity by
 538 studying the properties of the conditional and inverse probability density functions through
 539 the analysis of seismic catalogs. With these auxiliaries, the application of the Bayesian
 540 updating method to real seismic activity is expected to proceed while solving the lim-
 541 itation of seismic data.

542 **Appendix A Derivation of the conditional and inverse probability den-** 543 **sity functions for the uncorrelated time series**

First, we derive the conditional probability density function (Equation (15)) by sub-
 544 stituting Equations (12)–(14) into Equation (11). The denominator of Equation (11) is

$$\sum_{i=1}^{\infty} i \Psi_{mM}(i|\tau_M) = A_{\Delta m} \frac{\tau_M}{\langle \tau_M \rangle} + 1,$$

and the numerator is

$$\begin{aligned} \sum_{i=1}^{\infty} i \rho_{mM}(\tau_m|i, \tau_M) \Psi_{mM}(i|\tau_M) &= e^{-A_{\Delta m} \frac{\tau_M}{\langle \tau_M \rangle}} \delta(\tau_M - \tau_m) \\ &+ e^{-A_{\Delta m} \frac{\tau_m}{\langle \tau_M \rangle}} \frac{A_{\Delta m}}{\langle \tau_M \rangle} \sum_{i=0}^{\infty} (i+2) \frac{\left\{ A_{\Delta m} \frac{\tau_M}{\langle \tau_M \rangle} \left(1 - \frac{\tau_m}{\tau_M} \right) \right\}^i}{i!} e^{-A_{\Delta m} \frac{\tau_M}{\langle \tau_M \rangle} \left(1 - \frac{\tau_m}{\tau_M} \right)} \theta(\tau_M - \tau_m) \\ &= e^{-A_{\Delta m} \frac{\tau_M}{\langle \tau_M \rangle}} \delta(\tau_M - \tau_m) + e^{-A_{\Delta m} \frac{\tau_m}{\langle \tau_M \rangle}} \frac{A_{\Delta m}}{\langle \tau_M \rangle} \left\{ A_{\Delta m} \frac{\tau_M}{\langle \tau_M \rangle} \left(1 - \frac{\tau_m}{\tau_M} \right) + 2 \right\} \theta(\tau_M - \tau_m). \end{aligned}$$

544 Equation (15) is obtained by rearranging the above equations.

We confirm that Equation (2) with this conditional probability in its kernel has the
 exponential distribution (Equation (10)) as the solution. By dividing both sides of Equa-
 tion (2) by N_m and rewriting it using $N_M/N_m = \langle \tau_m \rangle / \langle \tau_M \rangle$ as well as Equation (15)

$$\begin{aligned} p_m(\tau_m) &= \frac{\langle \tau_m \rangle}{\langle \tau_M \rangle} \int_{\tau_m}^{\infty} \left[e^{-A_{\Delta m} \frac{\tau_M}{\langle \tau_M \rangle}} \delta(\tau_M - \tau_m) \right. \\ &\quad \left. + \frac{A_{\Delta m}}{\langle \tau_M \rangle} e^{-A_{\Delta m} \frac{\tau_m}{\langle \tau_M \rangle}} \left\{ A_{\Delta m} \frac{\tau_M - \tau_m}{\langle \tau_M \rangle} + 2 \right\} \theta(\tau_M - \tau_m) \right] p_M(\tau_M), \quad (\text{A1}) \end{aligned}$$

where the following general relation is used.

$$\frac{\tau_M}{\langle\langle\tau_m\rangle\rangle_{\tau_M}} = \sum_{i=1}^{\infty} i\Psi_{mM}(i|\tau_M).$$

We show that the r.h.s. of Equation (A1) is equivalent to the l.h.s., $p_m(\tau_m) = e^{-\frac{\tau_m}{\langle\tau_m\rangle}}/\langle\tau_m\rangle$. Substitute $p_M(\tau_M) = e^{-\frac{\tau_M}{\langle\tau_M\rangle}}/\langle\tau_M\rangle$ into the r.h.s. of Equation (A1) and note that $A_{\Delta m} + 1 = \langle\tau_M\rangle/\langle\tau_m\rangle$; the integral involving the delta function (R_1) is

$$R_1 = \frac{\langle\tau_m\rangle}{\langle\tau_M\rangle^2} e^{-\frac{\tau_m}{\langle\tau_m\rangle}}, \quad (\text{A2})$$

and the integral involving the step function (R_2) is

$$\begin{aligned} R_2 &= \frac{\langle\tau_m\rangle}{\langle\tau_M\rangle^3} A_{\Delta m} e^{-A_{\Delta m} \frac{\tau_m}{\langle\tau_M\rangle}} \int_{\tau_m}^{\infty} \left\{ A_{\Delta m} \frac{\tau_M - \tau_m}{\langle\tau_M\rangle} + 2 \right\} e^{-\frac{\tau_M}{\langle\tau_M\rangle}} d\tau_M \\ &= \frac{\langle\tau_m\rangle}{\langle\tau_M\rangle^2} A_{\Delta m} (A_{\Delta m} + 2) e^{-\frac{\tau_m}{\langle\tau_m\rangle}}. \end{aligned} \quad (\text{A3})$$

Therefore, the r.h.s. of Equation (A1) is shown to be equivalent to the l.h.s. of Equation (A1) as follows:

$$\begin{aligned} R_1 + R_2 &= \frac{\langle\tau_m\rangle}{\langle\tau_M\rangle^2} (1 + A_{\Delta m})^2 e^{-\frac{\tau_m}{\langle\tau_m\rangle}} \\ &= \frac{1}{\langle\tau_m\rangle} e^{-\frac{\tau_m}{\langle\tau_m\rangle}}. \end{aligned} \quad (\text{A4})$$

Second, we derive the inverse probability density function (Equation (16)). From Equation (15), the generalized probability density functions for the uncorrelated time series are derived as

$$\begin{aligned} z_m(\tau_m) &= \frac{\tau_m}{\langle\tau_m\rangle^2} e^{-\frac{\tau_m}{\langle\tau_m\rangle}}, \\ z_M(\tau_M) &= \frac{\tau_M}{\langle\tau_M\rangle^2} e^{-\frac{\tau_M}{\langle\tau_M\rangle}}, \\ z_{mM}(\tau_m|\tau_M) &= \frac{\tau_m}{\tau_M} e^{-A_{\Delta m} \frac{\tau_m}{\langle\tau_M\rangle}} \left[\delta(\tau_M - \tau_m) + \frac{A_{\Delta m}}{\langle\tau_M\rangle} \left\{ A_{\Delta m} \frac{\tau_M}{\langle\tau_M\rangle} \left(1 - \frac{\tau_m}{\tau_M} \right) + 2 \right\} \theta(\tau_M - \tau_m) \right]. \end{aligned}$$

545

Equation (16) is obtained by substituting the above equations in Equation (8).

Derivative of Equation (16) by τ_M is

$$\frac{\partial}{\partial\tau_M} p_{Mm}(\tau_M(> \tau_m)|\tau_m) = -\frac{\langle\tau_m\rangle^2}{\langle\tau_M\rangle^5} A_{\Delta m}^2 e^{\frac{\tau_m - \tau_M}{\langle\tau_M\rangle}} \left[\tau_M - \left\{ \tau_m + \langle\tau_M\rangle \left(1 - \frac{2}{A_{\Delta m}} \right) \right\} \right].$$

Therefore, the inverse probability density function has a peak at

$$\tau_M^{\max} = \tau_m + \langle\tau_M\rangle \left(1 - \frac{2}{A_{\Delta m}} \right),$$

under the condition of $\tau_M^{\max} > \tau_m$, which is equivalent to

$$\Delta m > \frac{\log_{10} 3}{b}.$$

Appendix B Derivation of Equation (24) from Equation (23)

The summation part in the r.h.s. of Equation (23) is

$$\begin{aligned}
 & \sum_{i=n}^{\infty} (i-n+1) \Psi_{mM}(i|\tau_M) \rho_{mM}(\tau_m^{(1)}|i, \tau_M) \prod_{j=2}^n \rho_{mM} \left(\tau_m^{(j)} | i-j+1, \tau_M - \sum_{k=1}^{j-1} \tau_m^{(k)} \right) \\
 &= \Psi_{mM}(n|\tau_M) \rho_{mM}(\tau_m^{(1)}|n, \tau_M) \prod_{j=2}^n \rho_{mM} \left(\tau_m^{(j)} | n-j+1, \tau_M - \sum_{k=1}^{j-1} \tau_m^{(k)} \right) \\
 &+ \sum_{i=n+1}^{\infty} (i-n+1) \Psi_{mM}(i|\tau_M) \rho_{mM}(\tau_m^{(1)}|i, \tau_M) \prod_{j=2}^n \rho_{mM} \left(\tau_m^{(j)} | i-j+1, \tau_M - \sum_{k=1}^{j-1} \tau_m^{(k)} \right).
 \end{aligned}$$

The first term on the r.h.s. of the above equation is transformed by substituting Equations (12)–(14) as

$$\begin{aligned}
 & \frac{[A_{\Delta m} \frac{\tau_M}{\langle \tau_M \rangle}]^{n-1}}{(n-1)!} e^{-A_{\Delta m} \frac{\tau_M}{\langle \tau_M \rangle}} \frac{(n-1)}{\tau_M} \left(\frac{\tau_M - \tau_m^{(1)}}{\tau_M} \right)^{n-2} \frac{(n-2)}{\tau_M - \tau_m^{(1)}} \left(\frac{\tau_M - \tau_m^{(1)} - \tau_m^{(2)}}{\tau_M - \tau_m^{(1)}} \right)^{n-3} \\
 & \dots \frac{\delta(\tau_M - \sum_{i=1}^n \tau_m^{(i)})}{\tau_M - \sum_{i=1}^{n-2} \tau_m^{(i)}} = \left(\frac{A_{\Delta m}}{\langle \tau_M \rangle} \right)^{n-1} e^{-A_{\Delta m} \frac{\tau_M}{\langle \tau_M \rangle}} \delta \left(\tau_M - \sum_{i=1}^n \tau_m^{(i)} \right). \quad (B1)
 \end{aligned}$$

The second term except the step function is also transformed as

$$\begin{aligned}
 & \sum_{i=n+1}^{\infty} (i-n+1) \frac{[A_{\Delta m} \frac{\tau_M}{\langle \tau_M \rangle}]^{i-1}}{(i-1)!} e^{-A_{\Delta m} \frac{\tau_M}{\langle \tau_M \rangle}} \frac{(i-1)}{\tau_M} \left(\frac{\tau_M - \tau_m^{(1)}}{\tau_M} \right)^{i-2} \\
 & \times \prod_{j=2}^n \frac{(i-j)}{\tau_M - \sum_{k=1}^{j-1} \tau_m^{(k)}} \left(\frac{\tau_M - \sum_{k=1}^j \tau_m^{(k)}}{\tau_M - \sum_{k=1}^{j-1} \tau_m^{(k)}} \right)^{i-j-1} \\
 &= \sum_{i=n+1}^{\infty} \frac{(i-n+1)}{(i-n-1)!} \left(\frac{A_{\Delta m}}{\langle \tau_M \rangle} \right)^{i-1} e^{-A_{\Delta m} \frac{\tau_M}{\langle \tau_M \rangle}} \left(\tau_M - \sum_{k=1}^n \tau_m^{(k)} \right)^{i-n-1} \\
 &= \sum_{i=0}^{\infty} \frac{i+2}{i!} \left(\frac{A_{\Delta m}}{\langle \tau_M \rangle} \right)^{i+n} e^{-A_{\Delta m} \frac{\tau_M}{\langle \tau_M \rangle}} \left(\tau_M - \sum_{k=1}^n \tau_m^{(k)} \right)^i \\
 &= \left(\frac{A_{\Delta m}}{\langle \tau_M \rangle} \right)^n e^{-A_{\Delta m} \frac{\sum_{i=1}^n \tau_m^{(i)}}{\langle \tau_M \rangle}} \sum_{i=0}^{\infty} \frac{i+2}{i!} \left\{ \frac{A_{\Delta m}}{\langle \tau_M \rangle} \left(\tau_M - \sum_{k=1}^n \tau_m^{(k)} \right) \right\}^i e^{-A_{\Delta m} \frac{\tau_M - \sum_{k=1}^n \tau_m^{(k)}}{\langle \tau_M \rangle}} \\
 &= \left(\frac{A_{\Delta m}}{\langle \tau_M \rangle} \right)^n e^{-A_{\Delta m} \frac{\sum_{i=1}^n \tau_m^{(i)}}{\langle \tau_M \rangle}} \left(A_{\Delta m} \frac{\tau_M - \sum_{i=1}^n \tau_m^{(i)}}{\langle \tau_M \rangle} + 2 \right). \quad (B2)
 \end{aligned}$$

Finally, Equation (24) is obtained by substituting Equations (B1) and (B2) in Equation (23), with the denominator of the r.h.s. of Equation (23)

$$\prod_{i=1}^n p_m(\tau_m^{(i)}) = \frac{1}{\langle \tau_m \rangle^n} e^{-\frac{\sum_{i=1}^n \tau_m^{(i)}}{\langle \tau_m \rangle}}.$$

Appendix C Another Bayesian updating method

In this appendix, we consider another method of Bayesian updating from the one introduced in §4; this method considers the consecutive lower intervals in the order of the appearance from the last event with magnitude greater than M . We derive the inverse probability density function for this updating method in the uncorrelated time series.

553 Let $N_{mM}^*(\tau_M, \tau_m^{(1)}, \dots, \tau_m^{(n)})$ be the total number of such upper intervals of length
 554 τ_M that include the consecutive lower intervals of lengths $\{\tau_m^{(1)}, \dots, \tau_m^{(n)}\}$ start from the
 555 leftmost one in the upper interval. Further, we denote the inverse probability density func-
 556 tion for this updating by $p_{Mm}^*(\tau_M | \tau_m^{(1)}, \dots, \tau_m^{(n)})$. We derive it by representing $N_{mM}^*(\tau_M, \tau_m^{(1)}, \dots, \tau_m^{(n)})$
 557 in two ways as follows:

First, we derive $N_{mM}^*(\tau_M, \tau_m^{(1)}, \dots, \tau_m^{(n)})$ by counting the total number of the up-
 per intervals of length τ_M that include the leftmost consecutive lower intervals of lengths
 $\{\tau_m^{(1)}, \dots, \tau_m^{(n)}\}$. The position of the first interval in the sequence of the consecutive lower
 intervals is fixed at the leftmost one in an upper interval, and therefore, the number of
 the sequence $\{\tau_m^{(1)}, \dots, \tau_m^{(n)}\}$ in the time series is

$$N_M \prod_{i=1}^n p_m(\tau_m^{(i)}) d\tau_m^n.$$

Among them, the number of sequences that belong to the same upper interval is

$$N_M \left(1 - \frac{\langle \tau_m \rangle}{\langle \tau_M \rangle}\right)^{n-1} \prod_{i=1}^n p_m(\tau_m^{(i)}) d\tau_m^n.$$

Therefore, the first representation is obtained as

$$\begin{aligned} & N_{mM}^*(\tau_M, \tau_m^{(1)}, \dots, \tau_m^{(n)}) \\ &= N_M \left(1 - \frac{\langle \tau_m \rangle}{\langle \tau_M \rangle}\right)^{n-1} \left\{ \prod_{i=1}^n p_m(\tau_m^{(i)}) \right\} p_{Mm}^*(\tau_M | \tau_m^{(1)}, \dots, \tau_m^{(n)}) d\tau_M d\tau_m^n. \end{aligned}$$

This equation is rewritten using Equation (10) in the explicit form as

$$\begin{aligned} & N_{mM}^*(\tau_M, \tau_m^{(1)}, \dots, \tau_m^{(n)}) \\ &= N_M \left(1 - \frac{\langle \tau_m \rangle}{\langle \tau_M \rangle}\right)^{n-1} \frac{1}{\langle \tau_m \rangle^n} e^{-\frac{\sum_{i=1}^n \tau_m^{(i)}}{\langle \tau_m \rangle}} p_{Mm}^*(\tau_M | \tau_m^{(1)}, \dots, \tau_m^{(n)}) d\tau_M d\tau_m^n. \quad (C1) \end{aligned}$$

Second, we derive $N_{mM}^*(\tau_M, \tau_m^{(1)}, \dots, \tau_m^{(n)})$ by counting the total number of con-
 secutive lower intervals that start from the leftmost one in the upper intervals of length
 τ_M . There is only one way for the sequence of consecutive lower intervals of lengths $\{\tau_m^{(1)}, \dots, \tau_m^{(n)}\}$
 to be involved in each of the $N_M p_M(\tau_M) d\tau_M$ upper intervals of length τ_M . The prob-
 ability of the occurrence of that sequence in the upper interval is, when $i(\geq n)$ -lower
 intervals are included in it

$$\rho_{mM}(\tau_m^{(1)} | i, \tau_M) \prod_{j=2}^n \rho_{mM} \left(\tau_m^{(j)} | i - j + 1, \tau_M - \sum_{k=1}^{j-1} \tau_m^{(k)} \right) d\tau_m^n.$$

Therefore, the second representation is obtained as

$$\begin{aligned} & N_{mM}^*(\tau_M, \tau_m^{(1)}, \dots, \tau_m^{(n)}) \\ &= N_M p_M(\tau_M) \sum_{i=n}^{\infty} \Psi_{mM}(i | \tau_M) \rho_{mM}(\tau_m^{(1)} | i, \tau_M) \prod_{j=2}^n \rho_{mM} \left(\tau_m^{(j)} | i - j + 1, \tau_M - \sum_{k=1}^{j-1} \tau_m^{(k)} \right) d\tau_M d\tau_m^n. \end{aligned}$$

This equation is rewritten in the explicit form using Equations (12)–(14) in the same way
 as in Appendix B.

$$\begin{aligned} & N_{mM}^*(\tau_M, \tau_m^{(1)}, \dots, \tau_m^{(n)}) = N_M \frac{1}{\langle \tau_M \rangle} e^{-\frac{\tau_M}{\langle \tau_M \rangle}} d\tau_M d\tau_m^n \left(\frac{A_{\Delta m}}{\langle \tau_M \rangle} \right)^{n-1} \\ & \times \left\{ e^{-A_{\Delta m} \frac{\tau_M}{\langle \tau_M \rangle}} \delta \left(\tau_M - \sum_{i=1}^n \tau_m^{(i)} \right) + \left(\frac{A_{\Delta m}}{\langle \tau_M \rangle} \right) e^{-A_{\Delta m} \frac{\sum_{i=1}^n \tau_m^{(i)}}{\langle \tau_M \rangle}} \theta \left(\tau_M - \sum_{i=1}^n \tau_m^{(i)} \right) \right\}. \quad (C2) \end{aligned}$$

Finally, $p_{Mm}^*(\tau_M|\tau_m^{(1)}, \dots, \tau_m^{(n)})$ is derived from Equations (C1) and (C2) as

$$\begin{aligned}
 & p_{Mm}^*(\tau_M|\tau_m^{(1)}, \dots, \tau_m^{(n)}) \\
 &= \frac{\langle \tau_m \rangle}{\langle \tau_M \rangle} \left\{ \frac{A_{\Delta m}}{\langle \tau_M \rangle} e^{-\frac{\tau_M - \sum_{i=1}^n \tau_m^{(i)}}{\langle \tau_M \rangle}} \theta \left(\tau_M - \sum_{i=1}^n \tau_m^{(i)} \right) + e^{-\frac{\tau_M - \sum_{i=1}^n \tau_m^{(i)}}{\langle \tau_m \rangle}} \delta \left(\tau_M - \sum_{i=1}^n \tau_m^{(i)} \right) \right\}.
 \end{aligned} \tag{C3}$$

558 This is different from Equation (24), which reflects the difference whether the position
 559 of lower intervals is specified.

560 Appendix D Derivation of Equation (29)

First, we substitute Equations (12)–(14) into Equation (28)

$$\begin{aligned}
 P^R(\tau_m|\tau_M) &= P^L(\tau_m|\tau_M) \\
 &= e^{-A_{\Delta m} \frac{\tau_M}{\langle \tau_M \rangle}} \delta(\tau_M - \tau_m) \\
 &\quad + \sum_{i=2}^{\infty} \frac{(i-1)}{\tau_M} \left(1 - \frac{\tau_m}{\tau_M}\right)^{i-2} \frac{\left(A_{\Delta m} \frac{\tau_M}{\langle \tau_M \rangle}\right)^{i-1}}{(i-1)!} e^{-A_{\Delta m} \frac{\tau_M}{\langle \tau_M \rangle}} \theta(\tau_M - \tau_m).
 \end{aligned}$$

In the above equation, the summation part of the term including the step function can be transformed as

$$\begin{aligned}
 & \sum_{i=2}^{\infty} \frac{(i-1)}{\tau_M} \left(1 - \frac{\tau_m}{\tau_M}\right)^{i-2} \frac{\left(A_{\Delta m} \frac{\tau_M}{\langle \tau_M \rangle}\right)^{i-1}}{(i-1)!} e^{-A_{\Delta m} \frac{\tau_M}{\langle \tau_M \rangle}} \\
 &= \frac{A_{\Delta m}}{\langle \tau_M \rangle} e^{-A_{\Delta m} \frac{\tau_M}{\langle \tau_M \rangle}} \sum_{i=0}^{\infty} \frac{\left\{A_{\Delta m} \frac{\tau_M}{\langle \tau_M \rangle} \left(1 - \frac{\tau_m}{\tau_M}\right)\right\}^i}{i!} e^{-A_{\Delta m} \frac{\tau_M}{\langle \tau_M \rangle}} \left(1 - \frac{\tau_m}{\tau_M}\right) \\
 &= \frac{A_{\Delta m}}{\langle \tau_M \rangle} e^{-A_{\Delta m} \frac{\tau_M}{\langle \tau_M \rangle}}.
 \end{aligned}$$

561 Finally, Equation (29) is obtained by rearranging the above equations.

562 Appendix E Derivation of Equation (34)

In this appendix, $P(\tau_m^{(1)}, \dots, \tau_m^{(l)}|\tau_M)$ is derived for the uncorrelated time series. First, we divide the summation in Equation (33) into two parts:

$$\begin{aligned}
 P(\tau_m^{(1)}, \dots, \tau_m^{(l)}|\tau_M) &= \sum_{i=l}^{\infty} \Psi_{mM}(i|\tau_M) \rho_{mM}(\tau_m^{(1)}|i, \tau_M) \prod_{j=2}^l \rho_{mM} \left(\tau_m^{(j)} | i - j + 1, \tau_M - \sum_{k=1}^{j-1} \tau_m^{(k)} \right) \\
 &= \Psi_{mM}(l|\tau_M) \rho_{mM}(\tau_m^{(1)}|l, \tau_M) \prod_{j=2}^l \rho_{mM} \left(\tau_m^{(j)} | l - j + 1, \tau_M - \sum_{k=1}^{j-1} \tau_m^{(k)} \right) \\
 &\quad + \sum_{i=l+1}^{\infty} \Psi_{mM}(i|\tau_M) \rho_{mM}(\tau_m^{(1)}|i, \tau_M) \prod_{j=2}^l \rho_{mM} \left(\tau_m^{(j)} | i - j + 1, \tau_M - \sum_{k=1}^{j-1} \tau_m^{(k)} \right)
 \end{aligned}$$

This equation is further rewritten by substituting Equations (12)–(14) in the same way as in Appendix B. The second term on the r.h.s. except for the step function is

$$\begin{aligned}
 & \sum_{i=l+1}^{\infty} \frac{\left(\frac{A_{\Delta m}}{\langle \tau_M \rangle}\right)^{i-1}}{(i-1)!} e^{-A_{\Delta m} \frac{\tau_M}{\langle \tau_M \rangle}} \frac{i-1}{\tau_M} \left(\frac{\tau_M - \tau_m^{(1)}}{\tau_M}\right)^{i-2} \\
 & \times \prod_{j=2}^l \frac{(i-j)}{\tau_M - \sum_{k=1}^{j-1} \tau_m^{(k)}} \left(\frac{\tau_M - \sum_{k=1}^j \tau_m^{(k)}}{\tau_M - \sum_{k=1}^{j-1} \tau_m^{(k)}}\right)^{i-j-1} \\
 & = \sum_{i=l+1}^{\infty} \frac{1}{(i-l-1)!} \left(\frac{A_{\Delta m}}{\langle \tau_M \rangle}\right)^{i-1} e^{-A_{\Delta m} \frac{\tau_M}{\langle \tau_M \rangle}} \left(\tau_M - \sum_{k=1}^l \tau_m^{(k)}\right)^{i-l-1} \\
 & = \sum_{i=0}^{\infty} \frac{1}{i!} \left(\frac{A_{\Delta m}}{\langle \tau_M \rangle}\right)^{i+l} e^{-A_{\Delta m} \frac{\tau_M}{\langle \tau_M \rangle}} \left(\tau_M - \sum_{k=1}^l \tau_m^{(k)}\right)^i \\
 & = \left(\frac{A_{\Delta m}}{\langle \tau_M \rangle}\right)^l e^{-A_{\Delta m} \frac{\sum_{i=1}^l \tau_m^{(i)}}{\langle \tau_M \rangle}} \sum_{i=0}^{\infty} \frac{\left\{\frac{A_{\Delta m}}{\langle \tau_M \rangle} \left(\tau_M - \sum_{k=1}^l \tau_m^{(k)}\right)\right\}^i}{i!} e^{-\frac{A_{\Delta m}}{\langle \tau_M \rangle} \left(\tau_M - \sum_{k=1}^l \tau_m^{(k)}\right)} \\
 & = \prod_{i=1}^l P_i(\tau_m^{(i)} | \tau_M),
 \end{aligned}$$

563 where $P_i(\tau_m^{(i)} | \tau_M) := \left(\frac{A_{\Delta m}}{\langle \tau_M \rangle}\right) e^{-A_{\Delta m} \frac{\tau_m^{(i)}}{\langle \tau_M \rangle}}$.

Therefore

$$P(\tau_m^{(1)}, \dots, \tau_m^{(l)} | \tau_M) = \left(\frac{A_{\Delta m}}{\langle \tau_M \rangle}\right)^{l-1} e^{-A_{\Delta m} \frac{\tau_M}{\langle \tau_M \rangle}} \delta\left(\tau_M - \sum_{i=1}^l \tau_m^{(i)}\right) + \prod_{i=1}^l P_i(\tau_m^{(i)} | \tau_M) \theta\left(\tau_M - \sum_{i=1}^l \tau_m^{(i)}\right).$$

Finally, because $\tau_M \geq \sum_{i=1}^l \tau_m^{(i)}$ holds for $l < n$ by the condition of Equation (26)

$$P(\tau_m^{(1)}, \dots, \tau_m^{(l)} | \tau_M) = \prod_{i=1}^l P_i(\tau_m^{(i)} | \tau_M).$$

564 Appendix F Derivation of Equation (39)

In this appendix, the approximation function of the inverse probability density function for the uncorrelated time series (Equation (39)) is derived. By substituting Equations (10), (15), and (34) into Equation (36)

$$\begin{aligned}
 & p_{MM}(\tau_M | \tau_m^{(1)}, \dots, \tau_m^{(n)}) \\
 & = \frac{\langle \tau_m \rangle}{\langle \tau_M \rangle} \frac{\left(A_{\Delta m} \frac{\tau_M}{\langle \tau_M \rangle} + 1\right)}{\left(A_{\Delta m} \frac{\langle \tau_m \rangle}{\langle \tau_M \rangle}\right)^{n-1}} \left[\prod_{i=1}^n \frac{e^{-A_{\Delta m} \frac{\tau_m^{(i)}}{\langle \tau_M \rangle}} \frac{A_{\Delta m}}{\langle \tau_M \rangle} \left\{A_{\Delta m} \frac{\tau_M}{\langle \tau_M \rangle} \left(1 - \frac{\tau_m^{(i)}}{\tau_M}\right) + 2\right\}}{\frac{1}{\langle \tau_m \rangle} e^{-\frac{\tau_m^{(i)}}{\langle \tau_m \rangle}} \left(A_{\Delta m} \frac{\tau_M}{\langle \tau_M \rangle} + 1\right)} \right] \frac{1}{\langle \tau_M \rangle} e^{-\frac{\tau_M}{\langle \tau_M \rangle}} \\
 & - \frac{\langle \tau_m \rangle}{\langle \tau_M \rangle} \frac{(n-1)}{\left(A_{\Delta m} \frac{\langle \tau_m \rangle}{\langle \tau_M \rangle}\right)^{n-1}} \left[\prod_{i=1}^n \frac{\left(\frac{A_{\Delta m}}{\langle \tau_M \rangle}\right) e^{-A_{\Delta m} \frac{\tau_m^{(i)}}{\langle \tau_M \rangle}}}{\frac{1}{\langle \tau_m \rangle} e^{-\frac{\tau_m^{(i)}}{\langle \tau_m \rangle}}} \right] \frac{1}{\langle \tau_M \rangle} e^{-\frac{\tau_M}{\langle \tau_M \rangle}}, \tag{F1}
 \end{aligned}$$

where the following relation is used.

$$\begin{aligned}
 \frac{\tau_M}{\langle \langle \tau_m \rangle \rangle_{\tau_M}} & = \sum_{i=1}^{\infty} i \Psi_{mM}(i | \tau_M) \\
 & = A_{\Delta m} \frac{\tau_M}{\langle \tau_M \rangle} + 1.
 \end{aligned}$$

The two products ($[\dots]$'s) in Equation (F1) are respectively transformed as

$$\begin{aligned} \prod_{i=1}^n \frac{\left(\frac{A_{\Delta m}}{\langle \tau_M \rangle}\right) e^{-A_{\Delta m} \frac{\tau_m^{(i)}}{\langle \tau_M \rangle}}}{\frac{1}{\langle \tau_m \rangle} e^{-\frac{\tau_m^{(i)}}{\langle \tau_m \rangle}}} &= \left(A_{\Delta m} \frac{\langle \tau_m \rangle}{\langle \tau_M \rangle}\right)^n \prod_{i=1}^n e^{-A_{\Delta m} \frac{\tau_m^{(i)}}{\langle \tau_M \rangle} + \frac{\tau_m^{(i)}}{\langle \tau_m \rangle}} \\ &= \left(A_{\Delta m} \frac{\langle \tau_m \rangle}{\langle \tau_M \rangle}\right)^n \prod_{i=1}^n e^{\frac{\tau_m^{(i)}}{\langle \tau_M \rangle}}. \end{aligned} \quad (\text{F2})$$

$$\begin{aligned} \prod_{i=1}^n \frac{e^{-A_{\Delta m} \frac{\tau_m^{(i)}}{\langle \tau_M \rangle}} \frac{A_{\Delta m}}{\langle \tau_M \rangle} \left\{ A_{\Delta m} \frac{\tau_M}{\langle \tau_M \rangle} \left(1 - \frac{\tau_m^{(i)}}{\tau_M}\right) + 2 \right\}}{\frac{1}{\langle \tau_m \rangle} e^{-\frac{\tau_m^{(i)}}{\langle \tau_m \rangle}} \left(A_{\Delta m} \frac{\tau_M}{\langle \tau_M \rangle} + 1 \right)} \\ = \left(A_{\Delta m} \frac{\langle \tau_m \rangle}{\langle \tau_M \rangle}\right)^n \left(\prod_{i=1}^n e^{-A_{\Delta m} \frac{\tau_m^{(i)}}{\langle \tau_M \rangle} + \frac{\tau_m^{(i)}}{\langle \tau_m \rangle}} \right) \left\{ \prod_{i=1}^n \frac{A_{\Delta m} \frac{\tau_M}{\langle \tau_M \rangle} + 1 - \left(A_{\Delta m} \frac{\tau_m^{(i)}}{\langle \tau_M \rangle} - 1 \right)}{A_{\Delta m} \frac{\tau_M}{\langle \tau_M \rangle} + 1} \right\} \\ = \left(A_{\Delta m} \frac{\langle \tau_m \rangle}{\langle \tau_M \rangle}\right)^n \left(\prod_{i=1}^n e^{\frac{\tau_m^{(i)}}{\langle \tau_M \rangle}} \right) \left\{ \prod_{i=1}^n \left(1 - \frac{\tau_m^{(i)} - \frac{\langle \tau_M \rangle}{A_{\Delta m}}}{\tau_M + \frac{\langle \tau_M \rangle}{A_{\Delta m}}} \right) \right\}. \end{aligned} \quad (\text{F3})$$

565 Finally, Equation (39) is derived by substituting Equations (F2) and (F3) into Equation
566 (F1).

567 Appendix G Relation between the inverse probability density func- 568 tion and its approximation function in the uncorrelated 569 time series

570 In this appendix, we discuss the relation between the inverse probability density
571 function (Equation (23)) and Equation (36), i.e., the approximations made on Equation
572 (23) that correspond to the assumptions made in §4.2 to derive Equation (36).

The summation in Equation (23) can be decomposed into

$$\begin{aligned} \sum_{i=n}^{\infty} (i - n + 1) \Psi_{mM}(i|\tau_M) \rho_{mM}(\tau_m^{(1)}|i, \tau_M) \prod_{j=2}^n \rho_{mM} \left(\tau_m^{(j)} | i - j + 1, \tau_M - \sum_{k=1}^{j-1} \tau_m^{(k)} \right) \\ = -(n-1) \sum_{i=n}^{\infty} \Psi_{mM}(i|\tau_M) \rho_{mM}(\tau_m^{(1)}|i, \tau_M) \prod_{j=2}^n \rho_{mM} \left(\tau_m^{(j)} | i - j + 1, \tau_M - \sum_{k=1}^{j-1} \tau_m^{(k)} \right) \\ + \sum_{i=n}^{\infty} i \Psi_{mM}(i|\tau_M) \rho_{mM}(\tau_m^{(1)}|i, \tau_M) \prod_{j=2}^n \rho_{mM} \left(\tau_m^{(j)} | i - j + 1, \tau_M - \sum_{k=1}^{j-1} \tau_m^{(k)} \right). \end{aligned} \quad (\text{G1})$$

573 The first term on the r.h.s. of Equation (G1) is equivalent to $-(n-1) \prod_{i=1}^n P_i$ (Ap-
574 pendix E), and then, this term formally coincides with the correction term in Equation
575 (36). Therefore, the second term corresponds to the kernel part (Equation (37)).

576 n -consecutive lower intervals must be included in only one upper interval. Under
577 this condition, three constraints are imposed on the lower intervals, which appear on the
578 l.h.s. of Equation (G1) as follows: (1) The number of lower intervals included in the up-
579 per interval must be larger than or equal to n . Then, the summation is taken in the range
580 of $i \geq n$. (2) The way to choose the n -consecutive intervals from the i -lower intervals
581 in an upper interval is only $(i - n + 1)$. If the first lower interval (or the leftmost one
582 in the sequence of the consecutive lower intervals) is in either remaining $(n-1)$ ways,
583 the sequence overflows from the upper interval. (3) The probability of the length of the
584 j -th interval in the consecutive lower intervals depends on the way other (k -th, $1 \leq k <$

585 j) lower intervals appear, i.e., it is dependent on the remained time $\tau_M - \sum_{k=1}^{j-1} \tau_m^{(k)}$ and
 586 number of pieces of lower intervals $(i - j + 1)$, $\rho_{mM} \left(\tau_m^{(j)} | i - j + 1, \tau_M - \sum_{k=1}^{j-1} \tau_m^{(k)} \right)$.

These constraints are relaxed in the derivation in §4.2. In the view in §4.2, the upper intervals of length τ_M are collected and the new time series is generated as shown in Figure 5. For this new time series, the only constraint imposed on the lower intervals is that they are included in the upper interval of length τ_M ; each interval is assumed to occur independently. Therefore, the three constraints are changed in the following manner: (1) The new time series is generated by gathering all upper intervals of length τ_M , regardless of the number of lower intervals included in it. In addition, the restriction on the range of the summation ($i \geq n$) does not make much sense because the consecutive lower intervals are not assumed to be within only one upper interval, i.e., it is expanded to $i \geq 1$. (2) The number of ways to choose the n -consecutive intervals from i -lower intervals is unchanged; this exceeds the above mentioned upper limit ($i - n + 1$) although such cases are subtracted by the first term on the r.h.s. of Equation (G1), i.e., the correction term in Equation (36). (3) The constraints imposed on the condition in ρ_{mM} are removed; because the probability of the length of j -th interval is only not affected by other lower intervals, the temporal part of ρ_{mM} is replaced by τ_M (Equation (G2)). In addition, the constraint on the number of division can be eliminated by taking the average (Equation (G3)).

$$\rho_{mM} \left(\tau_m^{(j)} | i - j + 1, \tau_M - \sum_{k=1}^{j-1} \tau_m^{(k)} \right) \approx \rho_{mM} \left(\tau_m^{(j)} | i - j + 1, \tau_M \right) \quad (\text{G2})$$

$$\begin{aligned} &\approx \frac{\sum_{i=1}^{\infty} i \Psi_{mM}(i | \tau_M) \rho_{mM}(\tau_m^{(j)} | i, \tau_M)}{\sum_{i=1}^{\infty} i \Psi_{mM}(i | \tau_M)} \quad (\text{G3}) \\ &= p_{mM}(\tau_m^{(j)} | \tau_M). \end{aligned}$$

587 Thus, ρ_{mM} 's are simply replaced by the conditional probability density functions.

In this way, the approximate view in §4.2 implies the following replacement in the exact inverse probability density function.

$$\begin{aligned} &\sum_{i=n}^{\infty} i \Psi_{mM}(i | \tau_M) \rho_{mM}(\tau_m^{(1)} | i, \tau_M) \prod_{j=2}^n \rho_{mM} \left(\tau_m^{(j)} | i - j + 1, \tau_M - \sum_{k=1}^n \tau_m^{(k)} \right) \\ &\approx \sum_{i=1}^{\infty} i \Psi_{mM}(i | \tau_M) \prod_{j=1}^n p_{mM}(\tau_m^{(j)} | \tau_M) \\ &= \frac{\tau_M}{\langle \langle \tau_m \rangle \rangle_{\tau_M}} \prod_{j=1}^n p_{mM}(\tau_m^{(j)} | \tau_M). \end{aligned}$$

588 Appendix H Distance between the inverse probability density function 589 and the inter-event time distribution

In this Appendix, we derive the distance between the inverse probability density function (Equation (24)) and the inter-event time distribution ($p_M(\tau_M)$)

$$D(p_{Mm} || p_M) := \int_T^{\infty} |p_{\theta}(\tau_M, T) - p_M(\tau_M)|^2 d\tau_M, \quad (\text{H1})$$

where

$$\begin{aligned} p_{\theta}(\tau_M, T) &= \frac{\langle \tau_m \rangle}{\langle \tau_M \rangle^2} \left(1 - \frac{\langle \tau_m \rangle}{\langle \tau_M \rangle} \right) e^{-\frac{\tau_M - T}{\langle \tau_M \rangle}} \left(A_{\Delta m} \frac{\tau_M - T}{\langle \tau_M \rangle} + 2 \right), \\ p_M(\tau_M) &= \frac{1}{\langle \tau_M \rangle} e^{-\frac{\tau_M}{\langle \tau_M \rangle}}. \end{aligned}$$

By substituting these functions in Equation (H1), the distance is derived as

$$D(p_{Mm}||p_M) = \frac{\langle \tau_M \rangle C_1^2}{4} + \frac{C_1 C_2(T)}{2} + \frac{C_2(T)^2}{2\langle \tau_M \rangle}, \quad (\text{H2})$$

where

$$C_1 = \frac{1}{\langle \tau_M \rangle} \left(1 - \frac{\langle \tau_m \rangle}{\langle \tau_M \rangle} \right)^2,$$

$$C_2(T) = 2 \frac{\langle \tau_m \rangle}{\langle \tau_M \rangle} \left(1 - \frac{\langle \tau_m \rangle}{\langle \tau_M \rangle} \right) - e^{-\frac{T}{\langle \tau_M \rangle}}.$$

Appendix I On the cause of the separation of $\langle D'(p_{Mm}^{\text{approx}}||p_M) \rangle$ and $\langle D''(p_{Mm}^{\text{approx}}||p_M) \rangle$ at large T

In this appendix, we examine the cause of the separation between $\langle D'(p_{Mm}^{\text{approx}}||p_M) \rangle$ and $\langle D''(p_{Mm}^{\text{approx}}||p_M) \rangle$ at long-elapsed time T . Let us compare Figure 7 to Figures S6(a) and (c) for $\mathcal{N} = 10^5$. The separation is suppressed compared to that shown in Figure 7, which indicates that the fluctuations in the spline functions of \mathbf{P}_1 caused by a relatively small number of samples in the calculation of \mathbf{P}_1 are suppressed by increasing the sample data. This leads to the reduction of errors in the calculations (44), and to the improvement of the calculation of distance in Equation (46).

In addition, we tested numerical updating with $\mathcal{N} = 10^5$ by excluding some larger columns of the matrix \mathbf{P}_1 , i.e., by using the following matrix \mathbf{P}'_1 with an integer l_c

$$\mathbf{P}'_1 = \left[[P_{1,jk}]_{j=j_{\min}^{(k)}, \dots, j_{\max}^{(k)}} \right]_{k=k_{\min}, \dots, k_{\max}-l_c}. \quad (\text{II})$$

For this \mathbf{P}'_1 , the interpolation and extrapolation procedures are conducted in the same way as in §5.1, and the numerical updating is executed.

Figures S6(b) and (d) show the results of the distance for such updating with (b) $\Delta\tau_M = 0.1$ and $l_c = 5$, and (d) $\Delta\tau_M = 0.025$ and $l_c = 20$. Compared to the results obtained using \mathbf{P}_1 in Figures S6(a) and (c), the separation is suppressed further. Combined with the results for the kernel part, these results suggest the following; the number of samples to calculate \mathbf{P}_1 is so small compared to that of the conditional probability (the number of sample is only one for an upper interval for \mathbf{P}_1 whereas all the lower intervals included in an upper interval are used as a sample to calculate the conditional probability), in particular for a large k , that its fluctuation becomes too large to compute the correction term precisely.

Acknowledgments

The idea of generalized probability density functions and the simplified relation (7) are by Y. Aizawa. We would like to thank Editage (www.editage.com) for English language editing. This work was supported by JST SPRING, Grant Number JPMJSP2110.

References

- Aizawa, Y., Hasumi, T., & Tsugawa, S. (2013). Seismic statistics. *Nonlinear Phenomena in Complex Systems*, 16(2), 116–130.
- Aizawa, Y., & Tsugawa, S. (2014). Aftershock cascade of the 3.11 earthquake (2011) in fukushima-miyagi area. In D. Matrasulov & H. E. Stanley (Eds.), *Nonlinear phenomena in complex systems: From nano to macro scale* (pp. 21–33). Dordrecht: Springer Netherlands.
- Bak, P., Christensen, K., Danon, L., & Scanlon, T. (2002). Unified scaling law for earthquakes. *Physical Review Letters*, 88(17), 178501.

- 623 Bottiglieri, M., de Arcangelis, L., Godano, C., & Lippiello, E. (2010). Multiple-time
624 scaling and universal behavior of the earthquake interevent time distribution.
625 *Physical Review Letters*, *104*(15), 158501.
- 626 Corral, A. (2004). Long-term clustering, scaling, and universality in the temporal oc-
627 currence of earthquakes. *Physical Review Letters*, *92*(10), 108501.
- 628 Gutenberg, B., & Richter, C. F. (1944). Frequency of earthquakes in california. *Bul-
629 letin of the Seismological Society of America*, *34*(4), 185–188.
- 630 Helmstetter, A., & Sornette, D. (2002). Subcritical and supercritical regimes in
631 epidemic models of earthquake aftershocks. *Journal of Geophysical Research:
632 Solid Earth*, *107*(B10), ESE 10-1-ESE 10-21. Retrieved from [https://agupubs
633 .onlinelibrary.wiley.com/doi/abs/10.1029/2001JB001580](https://agupubs.onlinelibrary.wiley.com/doi/abs/10.1029/2001JB001580) doi: [https://
634 doi.org/10.1029/2001JB001580](https://doi.org/10.1029/2001JB001580)
- 635 Helmstetter, A., & Sornette, D. (2003). Importance of direct and indirect trig-
636 gered seismicity in the etas model of seismicity. *Geophysical Research Letters*,
637 *30*(11). Retrieved from [https://agupubs.onlinelibrary.wiley.com/doi/
638 abs/10.1029/2003GL017670](https://agupubs.onlinelibrary.wiley.com/doi/abs/10.1029/2003GL017670) doi: <https://doi.org/10.1029/2003GL017670>
- 639 Lippiello, E., Corral, Á., Bottiglieri, M., Godano, C., & Arcangelis, L. (2012).
640 Scaling behavior of the earthquake intertime distribution: Influence of large
641 shockss and time scales in the omori law. *Physical Review E*, *86*(6), 066119.
- 642 Ogata, Y. (1988). Statistical models for earthquake occurrences and residual
643 analysis for point processes. *Journal of the American Statistical association*,
644 *83*(401), 9–27.
- 645 Ogata, Y. (1998). Space-time point-process models for earthquake occurrences. *An-
646 nals of the Institute of Statistical Mathematics*, *50*(2), 379–402.
- 647 Omori, F. (1894). On aftershocks of earthquakes. *The journal of the College of Sci-
648 ence, Imperial University of Tokyo, Japan*, *7*, 111–200.
- 649 Saichev, A., & Sornette, D. (2006). “universal” distribution of interearthquake times
650 explained. *Phys. Rev. Lett.*, *97*, 078501. Retrieved from [https://link.aps
651 .org/doi/10.1103/PhysRevLett.97.078501](https://link.aps.org/doi/10.1103/PhysRevLett.97.078501) doi: [10.1103/PhysRevLett.97
652 .078501](https://doi.org/10.1103/PhysRevLett.97.078501)
- 653 Scholz, C. H. (2002). *The mechanics of earthquakes and faulting*. Cambridge univer-
654 sity press.
- 655 Tanaka, H., & Aizawa, Y. (2017). Detailed analysis of the interoccurrence time
656 statistics in seismic activity. *Journal of the Physical Society of Japan*, *86*(2),
657 024004.
- 658 Tanaka, H., & Umeno, K. (2021). Bayesian updating for time-intervals of different
659 magnitude thresholds in marked point process and its application to time-
660 series of ETAS model. *ESS Open Archive*. Retrieved from [https://doi.org/
661 10.1002/essoar.10509635.1](https://doi.org/10.1002/essoar.10509635.1) doi: [10.1002/essoar.10509635.1](https://doi.org/10.1002/essoar.10509635.1)
- 662 Touati, S., Naylor, M., & Main, I. G. (2009). Origin and nonuniversality of the
663 earthquake interevent time distribution. *Physical Review Letters*, *102*(16),
664 168501.
- 665 Utsu, T. (1961). A statistical study on the occurrence of aftershocks. *Geophysical
666 Magazine*, *30*, 521–605.
- 667 Webb, D. J. (1974). The statistics of relative abundance and diversity. *Journal of
668 Theoretical Biology*, *43*(2), 277–291.